EXPERIMENTAL EVALUATION OF DESIGN PROCEDURES FOR FILLET WELDS TO HOLLOW STRUCTURAL SECTIONS

Jeffrey A. Packer [1]*, Ph. D., D. Sc., P. Eng., F. ASCE
Min Sun [2], Ph. D.
Kyle Tousignant[3], B.A.Sc

[1] Bahen/Tanenbaum Professor, Department of Civil Engineering, University of Toronto, 35 St. George Street, Toronto, ON, M5S 1A4, Canada.
[2] Structural Designer, Read Jones Christoffersen, 144 Front Street West, Toronto, ON, M5J 2L7, Canada.
[3] Ph.D. Candidate, Department of Civil Engineering, University of Toronto, 35 St. George Street, Toronto, ON, M5S 1A4, Canada.

* Corresponding author:
Phone: +1-416-978-4776
Fax: +1-416-978-7046
E-mail: jeffrey.packer@utoronto.ca

ABSTRACT

This paper discusses contemporary design procedures for fillet welds to Hollow Structural Sections (HSS) in several prominent design codes. The structural reliability associated with the "directional strength enhancement factor" contained in North American Specifications is examined, based on a set of laboratory tests on fillet-welded connections between HSS and rigid end-plates. A total of 33 connections, in which the welds had been designed to be the critical elements, were tested to failure by axial tension loading applied to the HSS members. The experimentally obtained weld strengths were compared to the predicted nominal strengths. The directional strength enhancement factor was found to lead to unsafe strength predictions, particularly for large weld sizes. Hence, a restriction on the use of this factor for fillet welds to HSS members, in North American steel design specifications, needs to be considered. The analysis also shows that Eurocode 3 fillet weld design provisions give conservative strength predictions.

Key Words: hollow structural section, rectangular hollow section, circular hollow section, connection, joint, welding, directional strength enhancement factor, fillet weld.

WELD DESIGN PHILOSOPHY FOR HOLLOW SECTION CONNECTIONS

For steel Hollow Structural Section (HSS) connections, recent standards and design guides (Wardenier et al. 2008; Packer et al. 2009; Packer et al. 2010; ISO 2013) have outlined two design approaches for proportioning welds:

(i) The weld can be sized to develop the yield strength of the connected branch. By setting the design strength of a fillet-welded joint equal to the yield strength of the connected branch member, the required effective weld throat (t_w) can be calculated in terms of the connected branch wall thickness (t). This will produce an upper bound on the weld size and hence be a conservative design procedure. Assuming an axially-loaded 90˚ T-connection between Rectangular Hollow Sections (RHS) made to ASTM A500 Grade C with matching electrodes, the results of method (i) for the design of fillet welds in various steel specifications/codes (CSA 2001; CEN 2005; AISC 2010; AWS 2010; CSA 2014) are listed in Table 1 (McFadden et al. 2013). Clearly, there is quite a disparity in fillet weld design criteria in these steel specifications/codes.

(ii) The weld can be sized so that it resists the actual forces in the connected branch member. This method requires using an effective length for the weld group, since extensive research (Frater and Packer 1992a, 1992b; Packer and Cassidy 1995; Packer and Sun 2011) has proven that the connected branch wall and the adjacent weld are generally loaded in a highly non-uniform manner around the branch, in a typical HSS-to-HSS connection.

Method (i) is appropriate if there is low confidence in the design forces in the branch, or if there is uncertainty regarding Method (ii), or if plastic stress redistribution is required in the connection. Method (i) permits a prequalified weld size to be easily determined. However, Method (ii) generally allows "downsizing" of a weld, and hence can lower the fabrication cost. It is particularly appropriate if the branch forces are low relative to the branch member capacity. AISC (2010) has adopted Method (ii) in Chapter K, for welds to RHS, by specifying a range of weld effective lengths for different connection configurations and loadings.

EFFECT OF LOADING ANGLE ON FILLET WELD BEHAVIOR

Starting from the 1930s, experimental and theoretical investigations have been conducted on the behavior of fillet welds as a function of direction of loading with respect to the weld axis, mostly on fillet welds in lap splice connections. The investigations that formed the basis of the modern fillet weld design equations in North American and European specifications are discussed in this section.

Development of North American Fillet Weld Design Criteria

It is well-known that as the angle of loading increases (from $\theta = 0^\circ$ for a longitudinally-loaded weld to $\theta = 90^\circ$ for a transversely-loaded weld), the strength of a fillet weld increases but its ductility decreases. Hence, within a fillet weld group, the longitudinal weld tends to have the lower bound of strength but the upper bound of ductility. Both American and Canadian steel design specifications, AISC 360-10 (AISC 2010) and CSA S16-14 (CSA 2014) recognize the influence of the loading angle on the fillet weld strength and ductility.

Early tests performed by Butler and Kulak (1971) indicate that strength ratios of fillet welds with loading angles of 30˚, 60˚, and 90˚ to longitudinal fillet welds ($\theta = 0^\circ$) are 1.34, 1.41 and 1.44, respectively. Based on experimental results, the analytical model developed by Kato and Morita (1974) predicts that a transverse fillet weld is 46% stronger than a longitudinal fillet weld of the same size and length, corresponding to a directional strength increase factor of 1.46. The fillet weld design equations in current American and Canadian steel design specifications originate from the research by Miazga and Kennedy (1989), where tests were performed on 42 fillet-welded lap splice connection specimens with 5 or 9 mm fillet welds, with the connection loaded in tension at angles to the weld axis from 0˚ to 90˚ in 15˚ increments. The strength of the fillet weld gradually increased to 1.50 times as the loading angle increased from 0˚ to 90˚. Based on the experimental results, Miazga and Kennedy (1989) proposed a method to predict the strength of fillet welds of different orientations based on a maximum shear stress failure criterion. Later, Lesik and Kennedy (1990) extended the work of Miazga and Kennedy (1989) and proposed a simplified equation which is a function only of the loading angle (i.e. the $(1.0 + 0.50\sin^{1.5}\theta)$ directional strength enhancement factor adopted in current American (AISC 2010) and Canadian (CSA

2014) specifications). It takes the form of a multiplier that is applied to the longitudinal fillet weld strength.

The test program of Miazga and Kennedy (1989) included connection specimens lap-spliced by fillet welds using the shielded metal arc welding (SMAW) process, which is not commonly used in industry for high-production welding. To re-evaluate the effectiveness of the ($1.0 + 0.50\sin^{1.5}\theta$) directional strength enhancement factor on the more prevalent flux-cored arc welding (FCAW) process, a series of investigations has been conducted by Ng et al. (2004a, 2004b) and Deng et al. (2006). Their reliability analyses showed that the design equations in the American and Canadian standards provide an adequate level of safety for both welding processes.

The tests performed by Ng et al. (2004a, 2004b) and Deng et al. (2006) consisted of concentrically loaded fillet-welded connections with all welds having the same loading orientation. However, fillet-welded connections commonly include welds at different orientations to the applied load, and the interaction between fillet welds of different loading angles remained unknown. Hence, Callele et al. (2009) tested 19 lap splice connections with multiple weld segments of different orientations. It was still found that the weld deformation capacity decreased as the loading angle increased (i.e. the maximum deformation capacity was obtained for a weld element loaded longitudinally; the minimum deformation capacity was obtained for a weld element loaded transversely). Due to this incompatibility, a transverse weld prevents a longitudinal weld from reaching its full strength before failure of the joint takes place. Hence, the tested weld groups possessed capacities significantly lower than the sum of the individual weld segment strengths. Therefore, Callele et al. (2009) proposed a simple method to account for this phenomenon conservatively by reducing the capacities of the more ductile welds by 0 to 15%. For example, for a weld group containing longitudinal and transverse welds, the longitudinal weld can only develop 85% of its full capacity before joint failure. This method has been adopted by current American and Canadian steel design specifications. In order to investigate the response of eccentrically loaded fillet welds, where the load is not in the plane of the weld group, Kanvinde et al. (2009) performed 60 bend tests on cruciform connection specimens. It was found that a bearing mechanism between the connected plates, which is not present for concentrically loaded joints, made an obvious contribution to the strength of fillet-welded joints under out-of-plane eccentric loading. Hence, the authors proposed a design approach which incorporated this beneficial effect.

Another important observation, based on the experimental evidence in the above research, is that the actual weld fracture plane does not always coincide with the theoretical throat. Since the theoretical effective throat thickness of a fillet weld is commonly defined, in various design specifications, as the height of the largest triangle that can be drawn using the two fusion faces and the underside of the weld (i.e. the shortest distance from the root to the face of the weld), the use of the theoretical effective throat thickness generally produces a conservative strength prediction.

However, the application of this "($1.0 + 0.50\sin^{1.5}\theta$) directional strength enhancement factor", also known as the "sinθ factor", in the design of fillet welds in HSS connections has been questioned since:

1. Unlike lap splice connections, fillet welds in many HSS connections have the welded attachment loaded in tension or bending, rather than in shear.
2. Since welding can only be done on the outside of a hollow section, fillet welds to HSS members will be subject to a local eccentricity. For example, tension loading in an attached wall will produce additional tensile stress at the root of the weld (see Fig. 1). In fact, relevant codes and standards recognize that eccentric loading on a fillet weld, causing tension at the weld root, may reduce weld capacity. For example, CSA W59 (2013a) Clause 4.1.3.3.2 even states that … "Single fillet and single partial joint penetration groove welds shall not be subjected to bending about the longitudinal axis of the weld if it produces tension at the root of the weld". EN 1993-1-8 (CEN 2005) Clause 4.12 states that such local eccentricity, producing tension at the root of the weld, should be taken into account, but it specifically notes that … "Local eccentricity need not be taken into account if a weld is used as part of a weld group around the perimeter of a structural hollow section". The basis for this Eurocode waiver is unknown. AWS D1.1 Section 2.6.2 (2010) states that, in the design of welded joints, the calculated stresses shall include those due to eccentricity caused by alignment of the connected parts, size and type of welds, but this Section pertains to connections which are "non-tubular".
3. It has been shown experimentally that the inclusion of the "sinθ factor" in the fillet weld strength calculation is non-conservative for RHS-to-RHS connections, when used in conjunction with current

AISC 360-10 Chapter K weld effective lengths/properties, because target reliability levels are not met (Packer and Sun 2011; McFadden and Packer 2013; McFadden et al. 2013; McFadden and Packer 2014; Tousignant and Packer 2015). As a result, AISC does not allow the "sinθ factor" to be used when the "effective length method" of AISC 360 Chapter K is employed for designing fillet welds in RHS connections (AISC 360-10 Commentary on K4).

An objective of this paper was to determine if the "sinθ factor" can be applied to fillet welds joining an HSS member to a rigid base, where the entire length of the weld would be effective (i.e. the AISC "effective length method" would not not applicable). Hence, in this investigation all connection specimens were made by welding HSS to rigid steel plates, to remove any influence of surface flexibility.

Development of European Fillet Weld Design Criteria

It can be concluded, based on the prior literature review, that although a fillet weld is simple in concept, the internal stress systems by which it transmits load are highly complex. The stresses over sections of the fillet weld can be highly irregular due to stress-raising effects, depending on a number of factors such as geometry of the weld, lack of or excessive penetration, geometry of the connection and residual stress. However, for design the strength of a fillet weld is often described by simplifying the force system, assuming a critical failure surface and distributing a mean stress over it. Same as the North American design criteria, Eurocode 3 (CEN 2005) considers the effective throat as the critical failure surface over which the stress due to the applied load is uniformly distributed. Different from the North American approach, Eurocode 3 requires the forces transferred by the fillet weld to be resolved into stress components in different directions ($\sigma_{\perp}$, $\tau_{\perp}$ and $\tau_{\parallel}$) over the effective throat area, which will be further discussed in the following section.

The European fillet weld design criteria originate from the research conducted by Jensen (1934) and Kist (1936) on fillet welds under consideration of constant deformation energy. Later, Vreedenburgh (1954) extended the tests carried out by Jensen (1934) and Kist (1936), from which the early European fillet weld design equation was developed. Later, IIW (1980) reported that the strength ratio of transverse to longitudinal fillet welds was $\sqrt{3}/\sqrt{2} = 1.22$. This ratio was recommended as a safe design value for the strength of transverse welds, although much higher ratios had been observed in the North American investigations. IIW suggested that such a difference was primarily due to friction and supporting effects between plates in the tested lap splice connections. The ratio of 1.22 is implied in the modern fillet weld design equation in EN1993-1-8 (CEN 2005), which was developed based on a von Mises hypothesis and verified experimentally by assessing the strength of fillet welds loaded at different angles. Tests in the above research showed that the strength of fillet welds under combined stresses, due to load applied at different angles, can be roughly represented by an ellipsoid in the $\sigma_{\perp}$, $\tau_{\perp}$, $\tau_{\parallel}$ space. Recent European research by Björk et al. (2012, 2014) has extended the fillet weld design rules to connections made of high and ultra-high-strength steel.

DESIGN SPECIFICATIONS

ANSI/AISC360 (AISC 2010)

In Section J, unless overmatched weld metal is used, the design strength ($V_r = \phi_w R_n$) of a single fillet weld is based on the assumed single limit state of shear rupture along the plane of the weld effective throat. This design strength is computed from the product of the weld metal nominal stress (F_{nw}) and the weld effective throat area (A_w), with a resistance factor ($\phi_w = 0.75$) applied. Hence, the nominal strength (R_n) is:

$$R_n = F_{nw} A_w \tag{1a}$$

$$F_{nw} = 0.60 X_u \tag{1b}$$

where X_u = ultimate strength of weld metal (F_{EXX} in AISC 360).

As an alternate, “for a linear weld group with a uniform leg size, loaded through the center of gravity” (i.e. “all elements are in a line or are parallel”, hence having the same deformation capacity), Section J2.4(a) permits the use of the directional strength enhancement factor (Equation 1c) for calculation of the weld metal nominal stress (F_{nw}).

$$F_{nw} = 0.60 X_u (1.0 + 0.50 \sin^{1.5}\theta) \tag{1c}$$

where θ = angle of loading measured from the weld longitudinal axis (in degrees).

As a special case of Section J2.4(a), Section J2.4(c) gives provisions for concentrically loaded fillet weld groups consisting of elements of multiple orientations. The nominal strength (R_n) of such joints, with both longitudinal and transverse fillet welds, can be determined as the higher of Equations 2a and 2b. This provision is to account for the deformation incompatibility between longitudinal and transverse fillet welds.

$$R_n = R_{nwl} + R_{nwt} \tag{2a}$$

$$R_n = 0.85R_{nwl} + 1.5R_{nwt} \tag{2b}$$

where R_{nwl} = total nominal strength of longitudinally loaded fillet welds; R_{nwt} = total nominal strength of transversely loaded fillet welds with F_{nw} calculated by Equation 1b.

CAN/CSA S16 (2001)

In the 2001 edition of the Canadian steel standard, the fillet weld design strength ($V_r = \phi_w R_n = 0.67R_n$) was taken as the lesser of two limit states: (i) shear rupture along the fusion face with the base metal (using Equation 3a), and (ii) shear rupture along the plane of the weld effective throat (using Equation 3b which allows use of the directional strength enhancement factor).

$$R_n = 0.67A_m F_u \tag{3a}$$

$$R_n = 0.67A_w X_u(1.0 + 0.50\sin^{1.5}\theta) \tag{3b}$$

where A_m = area of fusion face between weld and base metal; F_u = ultimate tensile strength of base metal. It should be noted that the design resistance (V_r) calculated using Equations 1a and 1c per AISC 360-10 is the same as that calculated using Equation 3b per CSA S16-01, because the terms (ϕ = 0.75)(0.60X_u) and (ϕ = 0.67)(0.67X_u) both equal 0.45 X_u.

CAN/CSA S16 (2014)

As with AISC 360 (2010), providing overmatched weld metal is not used, the 2014 Canadian standard specifies that the design strength ($V_r = \phi_w R_n = 0.67R_n$) of a fillet weld be determined from the limit state of shear rupture along the weld effective throat plane. The nominal strength of a joint is the sum of the nominal strengths of all the fillet weld elements having different orientations. The base metal strength check in CSA S16-01 was removed in CSA S16-09 and CSA S16-14 since, according to the research on fillet-welded lap splice connections by Ng et al. (2004a, 2004b), Deng et al. (2006), and Callele et al. (2009), the base metal strength check might prevent the designer from taking advantage of the full capacity of the weld. Another difference between CSA S16-01 (CSA 2001) and CSA S16-14 (CSA 2014) it that the latter considers the deformation incompatibility between welds with different orientations by introducing an "M_w factor".

$$R_n = 0.67 A_w X_u (1.0 + 0.50 \sin^{1.5}\theta) M_w \tag{4a}$$

$$M_w = \frac{0.85 + \theta_1/600}{0.85 + \theta_2/600} \tag{4b}$$

where θ & θ_1 = angle of loading (in degrees) of the weld element under consideration; θ_2 = angle of loading (in degrees) of the weld element in the joint that is nearest to 90˚; M_w = strength reduction factor to allow for the difference in deformation capacity of weld elements with different orientations (which is analogous to the "0.85" factor in Equation 2b).

EN1993-1-8 (2005)

Eurocode 3 (CEN 2005) specifies that the design resistance of a fillet weld be determined using either the Directional Method or the Simplified Method. For both methods, the assessment of the selected weld size is based on the ultimate strength of the base material (F_u), which can be correlated to the ultimate strength of the matching weld material using a "β_w correlation factor". Hence, it is generally safe if overmatched electrodes are used.

The Directional Method requires resolution of the resultant design force transmitted by a unit length of weld into components parallel and transverse to the longitudinal axis of the weld and normal and transverse to the plane of its throat. Assuming a design throat area of A_w, the product of the effective throat thickness and the unit weld length, the component forces can be used to calculate the component stresses (see Fig. 2) in the same directions. $\sigma_{\parallel}$, which is the normal stress parallel to the weld axis, is not considered when verifying the design resistance of the weld. The design resistance of the fillet weld is deemed sufficient if Equations 5a and 5b are satisfied along the entire length. Weld connecting elements with different material properties should be designed using the properties of the lower strength material.

$$[\sigma_{\perp}{}^2 + 3(\tau_{\perp}{}^2 + \tau_{\parallel}{}^2)]^{0.5} \leq F_u/(\beta_w\gamma_{M2}) \tag{5a}$$

$$\text{and } \sigma_{\perp} \leq 0.9F_u/\gamma_{M2} \tag{5b}$$

where $\sigma_{\perp}$ = normal stress perpendicular to the throat; $\tau_{\perp}$ = shear stress (in the plane of the throat) perpendicular to the axis of the weld; $\tau_{\parallel}$ = shear stress (in the plane of the throat) parallel to the axis of the weld; γ_{M2} = partial safety factor for the resistance of weld equal to 1.25; β_w = correlation factor for fillet welds.

Equation 5a can be simplified for 90° equal-legged welds to:

- For longitudinally-loaded welds (θ = 0˚)

$$V_r = \left(\frac{F_u}{\sqrt{3}\beta_w\gamma_{M2}}\right)t_w l_w \tag{6a}$$

- For transversely-loaded welds (θ = 90˚)

$$V_r = \left(\frac{F_u}{\sqrt{2}\beta_w\gamma_{M2}}\right)t_w l_w \tag{6b}$$

where V_r = design resistance of the fillet weld.

Thus, Eurocode 3 (CEN 2005) uses a relationship between the strength of a transverse weld to a longitudinal weld of $(\sqrt{3}/\sqrt{2}) = 1.22$, which is significantly less than the 1.50 factor used in current North American specifications (Equation 1c or Equation 4a).

The Simplified Method is an alternative to the Directional Method for fillet weld design. This method is independent of the orientation of the weld throat plane with respect to the applied force. In fact, it is a conservative alternative to Equation 5a. The Simplified Method assumes that all welds are loaded in pure shear parallel to the axis of the weld and the welds can then be proportioned using Equation 6a.

EXPERIMENTAL PROGRAM

Since a prime objective of this study was to determine if the "sinθ factor" is applicable when the entire length of a fillet weld in an HSS connection is effective (i.e. the influence of any surface flexibility of the base metal is absent), all connection specimens were made by welding either Circular Hollow Sections (CHS) or RHS to a rigid steel plate. A total of 33 HSS-to-plate connections with different weld sizes, and angles of either 60˚ or 90˚ between the HSS and plate (see Fig. 3), were designed and fabricated so that the connections would have a failure mode of weld fracture.

Geometric Properties

The measured geometric properties of all connection specimens are given in Tables 2 and 3. Different weld sizes, with the intended leg size ranging from 4 to 16 mm, were selected to investigate the validity of the "sinθ factor" comprehensively. Before testing, all "test welds" were manually ground into a triangular shape so that the weld leg sizes, as well as the theoretical effective throat size, could be accurately measured using a standard or skew-T fillet weld gage. For each RHS connection specimen, the cross-sectional dimensions of the weld were carefully measured at 20 positions around the footprint of the branch. For each CHS connection specimen, the cross-sectional dimensions of the weld were measured at uniform increments of 25-30 mm around the footprint of the branch. The averages of the theoretical effective throat thickness of the weld (t_w), and the weld leg length measured along the branch (w_b) and along the plate (w_p) are listed in Tables 2 and 3. The t_w-values in Tables 2 and 3 were determined from geometry (Equation 7), to take into account the effect of unequal weld leg sizes and the local dihedral angle (angle between the base metal fusion faces), ψ, on the orientation of the weld throat plane, and were used for analysis. Externally measured t_w-values were used for strength calculations to ensure that the "test welds" were critical during tension testing.

$$t_w = \frac{w_b w_p \sin \Psi}{\sqrt{w_b^2 + w_p^2 - 2 w_b w_p \cos \Psi}} \tag{7}$$

where w_b = weld leg measured along the HSS branch; w_p = weld leg measured along the plate.

After testing to failure, each connection was saw-cut (where possible) normal to the weld longitudinal axis at several positions around the branch footprint (two cuts per side for the RHS, and at the locations of the weld cross-sectional dimension measurements for the CHS). After surface polishing, all cross-sections were macro-etch examined, per ASTM E340-06 (2006), using a 10% nitral etchant solution. These cross-section profiles were then scanned into software programs so that the dimensions of the weld cross sections, in particular the effective throat thickness, could be accurately measured. The fillet weld throat thickness was taken as the height of the largest triangle that one could draw within the fusion face weld legs and the underside of the weld surface (see Fig. 4).

Internal weld-size measurements obtained by macro-etch examinations were in good agreement with the external measurements using the fillet weld gage. Hence, credence was given to the externally measured t_w-values in Tables 2 and 3 and the use of them in the following analysis. The length of weld (l_w in Tables 2 and 3) was based on the actual HSS perimeter and was hence measured along the root of the weld considering the angle between the HSS and plate.

Material Properties

All HSS were cold-formed to CAN/CSA G40.20/G40.21 Grade 350W (CSA 2013b). Tensile test coupons were taken from the RHS (at flat face locations away from the weld seam), the CHS (at 90°, 180° and 270° positions from the weld seam), as well as the intermediate rigid plates, and tested in accordance with ASTM A370 (2013) to determine the base metal mechanical properties. The average measured yield stress (F_y and F_{yp}, determined by the 0.2% strain offset method) and ultimate strength (F_u and F_{up}) of the HSS and plate materials are shown in Table 4.

Matching electrodes with a minimum guaranteed tensile strength of 490 MPa were used for all "test welds". For the material properties of the as-laid weld metals, all-weld-metal tensile coupons were made in accord with AWS D1.1 (2010). The average measured yield stress (F_{yw}, determined by the 0.2% strain offset method) and ultimate strength (X_u) of the weld metals are shown in Table 4.

Instrumentation

Strain gages (Group A) were mounted on the four faces of each RHS test specimen, well above the intermediate plate. These strain gages monitored any difference in strain between opposite RHS faces during testing, and hence any unintentional bending moments. No bending moment was measured in any test, hence all specimens were loaded only in axial tension.

To further confirm that weld elements were loaded uniformly, an additional set of eight strain gages (Group B) was placed on two adjacent RHS walls, just above the plate, for all test specimens. Typical load-strain relationships, at four different locations along one RHS face, are shown in Fig. 5. Such plots thus confirmed that all welds were loaded uniformly throughout each RHS connection test; hence the entire weld length could be considered as being effective.

For all CHS connection specimens, Group A and B consisted of four or eight strain gages mounted with uniform spacing around the CHS perimeter either well above the intermediate plate (Group A) or just above the intermediate plate (Group B). Similarly, it was found that all welds were uniformly loaded during the tests.

Linear Varying Differential Transformers (LVDTs) were also used to measure the load-displacement behavior of the connection region (see Fig. 6).

Connection Tests

Connection specimens were tested to failure in axial tension at a quasi-static load rate (see Fig. 6). Failure by weld rupture (see examples in Fig. 7) was achieved in all cases and the failure loads (P_u) of all specimens are given in Tables 2 and 3.

ANALYSIS AND RESULTS

For assessment of the various fillet weld design equations, analysis of test results has been performed using the measured weld effective throat size (i.e. the minimum distance between the weld root and the face of the triangular weld shape), which is the weld theoretical or effective throat size that would be used by a designer in calculations. This effective throat is indicated by the dashed line in Fig. 4. One should note that the typical fracture plane through the weld (solid line in Fig. 4) was generally closer to the HSS fusion face and has a longer failure line. The measured throat size was multiplied by the weld length to obtain the weld area, where the weld length was taken as the appropriate portion of the HSS perimeter (l_w in Tables 2 and 3), considering the RHS rounded corners. The use of this weld length provides a more scientific evaluation of the true “sinθ effect”, although most designers would just calculate the weld length for RHS from H_b and B_b dimensions (especially if the branch was inclined). The H_b and B_b approach will always give a longer weld length, thus generating a higher predicted strength, which will be un-conservative for design.

The experimentally obtained weld strengths (Tables 2 and 3) can then be compared to the predictions in accordance with each code/specification to assess whether a sufficient safety index (or safety margin) is obtained, both with and without the application of the fillet weld directional strength increase. For the four weld elements in the 60˚ RHS connections (Specimens 18 – 21), the strengths were calculated separately since the welds were oriented differently to the load. Similarly, the strengths of the six 60˚ CHS specimens were calculated by summing up "component" weld strengths along 25 mm – 30 mm lengths of weld (tributary to each weld cross-sectional dimension measurement).

AISC 360 (2010)

The predicted nominal strengths (R_n) of the test welds <u>without</u> using the directional strength enhancement factor are compared to the actual failure loads in Fig. 8. For the 90˚ connections, the nominal strengths were determined using Equations 1a and 1b; for the 60˚ connections, the nominal strengths were computed using Equation 2a. In this case, R_{nwl} is applied to the RHS oblique welds at locations a and b (see Fig. 3) based on their real oblique lengths, and to the 60º CHS welds based on their real elliptical length. Thus, all "sinθ effects" are omitted.

The predicted nominal strengths of the test welds <u>with</u> the directional strength enhancement factor are compared to the actual failure loads in Fig. 9. For the 90˚ connections, the nominal strengths were determined using Equations 1a and 1c; for the 60˚ RHS connections, the nominal strengths were computed using Equation 2b with the 1.5 factor for R_{nwt}. Equations 1a and 1b are used to calculate R_{nwt} since the directional strength increase is already accounted for by the 1.5 term. Equations 1a and 1c are used to calculate R_{nwl} to account for the directional strength increase factor for the 60˚ oblique welds. Also, R_{nwl} is multiplied by 0.85 (similar to M_w in Equation 3a per CSA S16-14) to account for the difference in deformation capacity between the oblique and transverse weld elements. (Theoretically, the 0.85 term should be larger since the 0.85 value applies to longitudinal welds). For the 60˚ CHS connections, Equations 1a, 1b, and 1c were used to compute the strength of each weld component. The 0.85 term in Equation 2b, which could technically apply – since the connection encompasses weld components with multiple orientations – was deemed too general for this situation, and omitted from the analysis.

CAN/CSA S16 (2014)

The predicted nominal strengths of the test welds without and with the "sinθ factor" are computed using Equations 4a and 4b, and are compared to the actual failure loads in Figs. 10 and 11. The "M_w factor" (Equation 4a), akin to the 0.85 term in Equation 2b, is continuous for CHS joints with respect to θ, and there was hence a rational basis to apply it to the 60° CHS connections. The value of θ used in both the sinθ factor and M_w factor to compute each component strength of a CHS joint was determined by numerical integration of a $\theta(l_w)$ function, which was derived using vector calculus.

CAN/CSA S16 (2001)

The predicted nominal strength of each welded joint without the "sinθ factor" was taken as the least of the limit states of: (i) shear rupture along the fusion face along the HSS branch (using F_u, w_b and Equation 3a), (ii) shear rupture along the fusion face along the intermediate plate (using F_{up}, w_p and Equation 3a), and (iii) shear rupture along the weld effective throat plane (using X_u, t_w and Equation 3b without the directional strength enhancement factor). The predicted nominal strength of each welded joint with the "sinθ factor" was determined by repeating the above procedures, with the directional strength enhancement factor in Equation 3b included.

All predictions per CSA S16-01 are compared to the actual failure loads in Figs. 12 and 13. When the "sinθ factor" is not used (Fig. 12), the predicted nominal strengths of nearly all of the 90° HSS connections (16 of 17 RHS connections and 6 of 6 CHS connections) are governed by the limit state of shear rupture along the weld effective throat, and all but one of the 60° HSS connections are governed by the limit state of shear rupture along the fusion face with the base metal at some location along the weld length. When the "sinθ factor" is included in the calculation (Fig. 13), the nominal strengths of all connections are governed by the limit state of shear rupture along the fusion face with the base metal at some location along the weld length.

EN1993-1-8 (2005)

Following the European fillet weld design criteria, the capacity of the tested fillet-welded joints was calculated using the stress components on the theoretical throat plane, as illustrated in Fig. 2. The design strength of the weld joint in all RHS and CHS connections was determined using Equations 8a to 8e, assuming a theoretical angle between the planes of the effective throat and the fusion face, γ, determined from the weld geometry and hence taking into account the effect of unequal weld leg sizes and the local dihedral angle on the orientation of the weld throat plane. Although a more accurate comparison between tested and calculated strengths may be conducted by measuring the actual angle between the planes of the effective throat and the fusion face, the theoretical angle is used since it was not possible to perform internal weld geometry measurement via sectioning on all connection specimens. Equation 5b was satisfied in all cases. The correlation factor for fillet welds, β_w, was taken as 0.9 according to Table 4.1 in EN1993-1-8 (CEN 2005) for both cold-formed hollow sections (to EN10219) and hot-finished hollow sections (to EN10210), for grade S355 (HSS with a nominal yield strength of 355 MPa). Since the target safety (reliability) index for this Eurocode method is unknown, a comparison is performed against the limit states design resistance, including the partial safety factor, γ_{M2}.

$$\tau_{\parallel} = \frac{P_u \cos\theta}{t_w l_w} \tag{8a}$$

$$\sigma_{\perp} = \frac{P_u \cos\gamma}{t_w l_w} \tag{8b}$$

$$\tau_{\perp} = \frac{P_u \sin\gamma}{t_w l_w} \tag{8c}$$

$$\text{Comparison stress } = [{\sigma_{\perp}}^2 + 3({\tau_{\perp}}^2 + {\tau_{\parallel}}^2)]^{0.5} \leq F_u/(\beta_w \gamma_{M2})$$

$$= \frac{P_u}{t_w l_w}[\cos^2\gamma + 3(\sin^2\gamma + \cos^2\theta)]^{0.5} \leq F_u/(\beta_w \gamma_{M2}) \tag{8d}$$

$$V_r = \max. P_u = \left(\frac{F_u}{\beta_w \gamma_{M2}}\right)\frac{1}{[\cos^2\gamma + 3(\sin^2\gamma + \cos^2\theta)]^{0.5}} t_w l_w \tag{8e}$$

All calculated design strengths are compared to the actual strengths in Fig. 14, which shows that EN1993-1-8 produces safe predictions for all tested weld joints. The average actual-strength-to-design-strength ratios for the RHS and CHS connections are 1.805 and 2.45, respectively (with an average of 2.04 overall).

Evaluation of Directional Strength Enhancement Factor

To determine if sufficient safety margins are achieved in the correlations presented in Figs. 8 – 13, (the AISC 360 Specification Commentary Chapter B stipulates a minimum target safety index (β) of 4.0, while the CSA S16 Annex B requires a β of 4.5), a simplified reliability analysis can be performed in which the resistance factor "ϕ_w" is given by (Fisher et al. 1978; Ravindra and Galambos 1978):

$$\phi_w = m_R \exp(-\alpha\beta COV) \tag{9}$$

where m_R = mean of the actual strength-to-nominal strength ratio; COV = coefficient of variation of this ratio; and α = coefficient of separation taken to be 0.55 (Ravindra and Galambos 1978). The calculated m_R, COV, ϕ_w, and β values are shown in Figs. 8 – 13.

For the predicted nominal strengths by AISC 360-10, <u>without</u> the directional strength enhancement factor (Fig. 8), the application of Equation 9 produces $\phi_w = 0.757 \geq 0.75$ as specified by AISC 360-10 for fillet welds. Alternatively, if $\phi_w = 0.75$ is used to calculate the design strength, an implied safety index of 4.06 is achieved. Thus, the prediction method is conservative. Similarly, the predicted nominal strengths by CSA S16-14 <u>without</u> the directional strength enhancement factor (Fig. 10) can be deemed approximately safe since, although the calculated $\phi_w = 0.629 < 0.67$ as specified by CSA S16-14, the implied safety index, $\beta = 4.08$, is close to the target safety index required by CSA S16-14 and greater than that required by AISC 360.

However, the predicted nominal strengths by AISC 360-10 and CSA S16-14 <u>with</u> the directional strength enhancement factors (Figs. 9 and 11) are unsafe since the calculated ϕ_w values (0.519 and 0.419, respectively) are much lower than the corresponding specified resistance factor values (0.75 and 0.67, respectively for AISC and CSA). Viewed another way, the implied safety indices (indicated by β on Figs. 9 and 11) are well below the target safety indices for AISC and CSA.

As shown in Figs. 12 and 13, the calculated ϕ_w-values for CSA S16-01 without and with the directional strength enhancement factor, using $\beta = 4.5$, are 0.721 and 0.657. CSA S16-01 (Fig. 13) is noticeably more conservative than CSA S16-14 (Fig. 11) with the directional strength enhancement factor. It is interesting to note that CSA S16-01, where base metal fusion failure is included as a limit state check, virtually meets the required weld resistance factor both without and with the directional strength enhancement factor (0.721 and 0.657, respectively, versus 0.67) (Figs. 12 and 13).

INFLUENCE OF WELD SIZE

One must bear in mind that the strength of a fillet weld is also influenced by the amount of weld root penetration. Small and large fillet welds both tend to have the same amount of root penetration; for large welds with multiple passes the root penetration is generally determined by just the root pass. In laboratory tests, the strength of small fillet welds will therefore be raised proportionally more than for large fillet welds, by the root penetration. The effect of this aid is generally linear (see Fig. 15), and the magnitude of the so-called "weld size effect" varies depending on the prediction model investigated. No trend is observed for the branch cross-sectional slenderness (Fig. 16). Since most laboratory research on weld-critical joints involves fairly small welds (because a weld fracture failure mode is sought), it should be noted that the results obtained would actually be more favorable than those from large-weld tests.

CONCLUSIONS

A total of 33 HSS-to-plate, weld-critical connections have been tested to failure under axial tension loading. The design methods for fillet welds to HSS members given in CSA S16-01, EN1993-1-8:2005, AISC 360-10 and CSA S16-14 have been assessed by comparing the actual fillet weld strengths to the predicted strengths. It can be concluded from this work that:

1. The Directional Method in Eurocode 3 produces safe strength predictions for fillet welds to HSS. Hence, the Simplified Method is even more conservative.

2. When the ($1.0 + 0.50\sin^{1.5}\theta$) directional strength enhancement factor is not included in the strength calculation of fillet welds to HSS, the equations in both the current American and Canadian specifications can be used with adequate safety (reliability) indices being achieved.
3. Restrictions need to be placed in current North American steel design codes on the use of such a fillet weld directional strength enhancement factor in HSS connections. It should be noted that the directional strength enhancement factor was developed based on tests on fillet welds in lap splice connections. According to this investigation of fillet welds in HSS connections, strength calculation including a directional strength enhancement factor leads to predictions which do not have a sufficient safety margin, even when it is not used in conjunction with the "effective length method" of AISC 360 Chapter K.
4. The relative strength (per unit throat thickness) of small fillet welds is considerably greater than large fillet welds.
5. CHS-to-plate specimens generally exhibited higher average strengths than did RHS-to-plate specimens.
6. A more rigorous reliability analysis, including the mean values and variations in actual-to-nominal ultimate strength of typical weld metal (X_u), if available, may indicate that a higher safety margin is achieved by North American fillet weld design models, since the actual ultimate strength of weld metal is consistently higher than nominal.

ACKNOWLEDGMENTS

Financial support has been provided by the American Institute of Steel Construction (AISC) and the Natural Sciences and Engineering Research Council of Canada (NSERC). Appreciation is extended to Atlas Tube for providing the HSS, to Walters Group Inc. and Kubes Steel for fabricating the connection specimens, and to Dr. G. S. Frater, Mr. P. Oatway, and Ms. J. Lu for their laboratory contributions.

REFERENCES

American Institute of Steel Construction (AISC). (2010). "Specification for structural steel buildings." *ANSI/AISC 360-10*, Chicago, IL.

American Society for Testing and Materials (ASTM). (2006). "Standard test method for macroetching metals and alloys." *ASTM E340-06*, West Conshohocken, PA.

American Society for Testing and Materials (ASTM). (2013). "Standard test methods and definitions for mechanical testing of steel products." *ASTM A370-13*, West Conshohocken, PA.

American Welding Society (AWS). (2010). "Structural welding code – Steel, 22nd. ed." *ANSI/AWS D1.1/D1.1M:2010*, Miami, FL.

Björk, T., Toivonen, J. and Nykänen, T. (2012). "Capacity of fillet welded joints made of ultra high-strength steel." *Welding in the World*, 56(3-4), 71-84.

Björk, T., Penttilä, T. and Nykänen, T. (2014). "Rotation capacity of fillet weld joints made of high-strength steel." *Welding in the World*, 58(6), 853-863.

Butler, L. J., and Kulak, G. L. (1971). "Strength of fillet welds as a function of direction of load." *Weld. J. Welding Research Supplement*, 50(5), 231-234.

Callele, L. J., Driver, R. G. and Grondin, G. Y. (2009). "Design and behavior of multi-orientation fillet weld connections." *Eng. J. AISC*, 46(4), 257-272.

Canadian Standards Association (CSA). (2001). "Limit states design of steel structures." CAN/*CSA S16-01*, Toronto, Canada.

Canadian Standards Association (CSA). (2013a). "Welded steel construction (metal arc welding)." *CSA W59-13*, Toronto, Canada.

Canadian Standards Association (CSA). (2013b). "General requirements for rolled or welded structural quality steel/structural quality steel." *CAN/CSA-G40.20-13/G40.21-13*, Toronto, Canada.

Canadian Standards Association (CSA). (2014). "Design of steel structures." *CSA S16-14*, Toronto, Canada.

Comité Européen de Normalisation (CEN). (2005). "Eurocode 3: Design of steel structures – Part 1-8: Design of joints." *EN 1993-1-8:2005*, Brussels, Belgium.

Deng, K., Grondin, G. Y. and Driver, R. G. (2006). "Effect of loading angle on the behavior of fillet welds." *Eng. J. AISC*, 43(1), 9-23.

Fisher, J. W., Galambos, T. V., Kulak, G. L. and Ravindra, M. K. (1978). "Load and resistance factor design criteria for connectors." *J. Struct. Div. ASCE*, 104(9), 1427-1441.

Frater, G. S. and Packer, J. A. (1992a). "Weldment design for RHS truss connections. I: Applications." *J. Struct. Eng. ASCE*, 118(10), 2784-2803.

Frater, G. S. and Packer, J. A. (1992b). "Weldment design for RHS truss connections. II: Experimentation." *J. Struct. Eng. ASCE*, 118(10), 2804-2820.

International Institute of Welding (IIW). (1980). "Deformation curves of fillet welds." *Document XV-467-80*, Commission XV, London, England.

International Organization for Standardization (ISO). (2013). "Static design procedure for welded hollow section joints – Recommendations." *ISO 14346:2013 (E)*, Geneva, Switzerland.

Jensen, C. D. (1934). "Combined stresses in fillet welds." *Amer. Weld. Soc. J.*, 13(2), 17-21.

Kanvinde, A. M., Grondin, G. Y., Gomez, I. R. and Kwan, Y. (2009). "Experimental investigation of fillet-welded joints subjected to out-of-plane eccentric loads." *Eng. J. AISC*, 46(3), 197-212.

Kato, B. and Morita, K. (1974). "Strength of transverse fillet welded joints." *Weld. J. Welding Research Supplement*, 53(2), 59-64.

Kist, N. C. (1936). "Berechnung der schweißnähte unter berücksichtigung konstanter gestaltänderungsenergie / Calculation of welds under consideration of constant deformation energy." *Vorbericht 2, Kongress Int. Ver. für Brückenbau und Hochbau*, Berlin, Germany.

Lesik, D. F. and Kennedy, D. J. (1990). "Ultimate strength of fillet welded connections loaded in plane." *Can. J. Civ. Eng.*, 17(1), 55-67.

McFadden, M. R. and Packer, J. A. (2013). "Effective weld properties for RHS-to-RHS moment T-connections." Phase 1 Report to the American Institute of Steel Construction, University of Toronto, Toronto, Canada.

McFadden, M. R., Sun, M. and Packer, J. A. (2013). "Weld design and fabrication for RHS connections." *Steel Construction – Design and Research*, 6(1), 5-10.

McFadden, M. R. and Packer, J. A. (2014). “Effective weld properties for hollow structural section T-connections under branch in-plane bending.” *Eng. J. AISC*, 51(4), 247-266.

Miazga, G. S. and Kennedy, D. J. (1989). “Behaviour of fillet welds as a function of the angle of loading.” *Can. J. Civ. Eng.*, 16(4), 583-599.

Ng, A. K. F., Deng, K., Grondin, G. Y. and Driver, R. G. (2004a). “Behavior of transverse fillet welds: experimental program.” *Eng. J. AISC*, 41(2), 39-54.

Ng, A. K. F., Driver, R. G. and Grondin, G. Y. (2004b). “Behavior of transverse fillet welds: parametric and reliability analyses.” *Eng. J. AISC*, 41(2), 55-67.

Packer, J. A. and Cassidy, C. E. (1995). “Effective weld length for HSS T, Y, and X connections.” *J. Struct. Eng. ASCE*, 121(10), 1402-1408.

Packer, J. A., Wardenier, J., Zhao, X. L., van der Vegte, G. J. and Kurobane, Y. (2009). “Design guide for rectangular hollow section (RHS) joints under predominantly static loading.” *Design Guide No. 3, 2nd. ed.*, CIDECT, Geneva, Switzerland.

Packer, J. A., Sherman, D. R. and Leece, M. (2010). “Hollow structural section connections.” *Steel Design Guide No. 24*, AISC, Chicago, IL.

Packer, J. A. and Sun, M. (2011). “Weld design for rectangular HSS connections.” *Eng. J. AISC*, 48(1), 31-48.

Ravindra, M. K. and Galambos, T. V. (1978). “Load and resistance factor design for steel.” *J. Struct. Div. ASCE*, 104(9), 1337-1353.

Tousignant, K. and Packer, J.A. (2015). “Weld effective lengths for rectangular HSS overlapped K-connections.” *Eng. J. AISC*, 52(4), 259-282.

Vreedenburgh, G. G. J. (1954). “New principles for the calculation of welded joints.” *Weld. J.*, 33(8), 743-751.

Wardenier J., Kurobane, Y., Packer, J. A., van der Vegte, G. J. and Zhao, X. L. (2008). “Design guide for circular hollow section (CHS) joints under predominantly static loading.” *Design Guide No. 1, 2nd. ed.*, CIDECT, Geneva, Switzerland.

NOTATION

The following symbols are used in this paper:

A_m	=	area of fusion face between weld and base metal
A_w	=	effective throat area of weld
B_b	=	overall width of RHS branch member
CHS	=	circular hollow section
COV	=	coefficient of variation
e	=	eccentricity
F_{nw}	=	nominal stress of weld metal
F_u	=	ultimate strength of RHS
F_{up}	=	ultimate strength of plate
F_y	=	yield stress of RHS
F_{yp}	=	yield stress of plate
F_{yw}	=	yield stress of weld metal
H_b	=	overall height of RHS branch member
HSS	=	hollow structural section
l_w	=	total length of weld
m_R	=	mean of ratio: (actual strength) / (nominal strength)
M_w	=	strength reduction factor to allow for the variation in deformation capacity of weld elements with different orientations
P	=	applied force
P_u	=	ultimate strength of connection at failure
RHS	=	rectangular hollow section
R_n	=	nominal strength
R_{nwl}	=	total nominal strength of longitudinally loaded fillet welds
R_{nwt}	=	total nominal strength of transversely loaded fillet welds (without "sin θ" factor applied)
t	=	wall thickness of RHS

t_p	=	thickness of intermediate plate
t_w	=	effective throat thickness of weld
V_r	=	design shear resistance
w_b	=	weld leg length measured along the HSS branch
w_p	=	weld leg length measured along the plate
X_u	=	ultimate strength of weld metal
α	=	coefficient of separation
β	=	safety (reliability) index
β_w	=	correlation factor for fillet welds
γ	=	theoretical angle between the planes of the effective throat and the fusion face
ϕ_w	=	resistance factor for weld metal
Ψ	=	local dihedral angle (angle between the base metal fusion faces)
θ	=	angle of loading measured from the weld longitudinal axis for fillet weld strength calculation (in degrees)
θ_1	=	angle of loading (in degrees) of the weld element under consideration
θ_2	=	angle of loading (in degrees) of the weld element in the joint that is nearest to 90˚
$\sigma_\perp$	=	normal stress perpendicular to the throat
$\sigma_\parallel$	=	normal stress parallel to the axis of the weld
$\tau_\perp$	=	shear stress (in the plane of the throat) perpendicular to the axis of the weld
$\tau_\parallel$	=	shear stress (in the plane of the throat) parallel to the axis of the weld
γ_{M2}	=	partial safety factor of 1.25 for the resistance of weld in EN1003-1-8:2005

LIST OF FIGURE CAPTIONS

Table 1. Comparison of fillet weld effective throats required to develop the yield resistance of a connected RHS branch member wall (McFadden et al. 2013)

Specification or code	t_w
ANSI/AISC 360-10 Table J2.5 (AISC 2010)	1.43 t
AWS D1.1/D1.1M: 2010 Clause 2.25.1.3 and Fig. 3.2 (AWS 2010)	1.07 t
CAN/CSA S16-01 Clause 13.13.2.2 (CSA 2001)	1.14 t
CSA S16-14 Clause 13.13.2.2 (CSA 2014)	0.95 t
EN1993-1-8: Directional method (CEN 2005)	1.28 t
EN1993-1-8: Simplified method (CEN 2005)	1.57 t

*This table assumes an axially-loaded 90˚ T-connection between RHS made to ASTM A500 Grade C with matching electrodes.

Table 2. Measured geometric properties and connection failure loads for RHS-to-plate specimens

Spec. No.	Angle between RHS and Plate	RHS Designation	t_p [mm]	l_w [mm]			Average of t_w [mm]			Average of w_b [mm]			Average of w_p [mm]			P_n [kN]
1	90°	127x127x8.0	25.0	481			3.6			5.5			4.8			831
2	90°	127x127x8.0	25.0	481			5.9			8.3			8.4			1166
3	90°	127x127x8.0	25.0	481			4.7			7.1			6.4			1235
4	90°	127x127x8.0	25.0	481			5.7			10.9			6.7			1311
5	90°	178x178x13.0	25.0	668			6.4			9.3			8.8			2433
6	90°	178x178x13.0	25.0	668			8.6			13.3			11.3			2574
7	90°	178x178x13.0	25.0	668			6.2			10.1			7.8			2525
8	90°	178x178x13.0	25.0	668			7.1			11.8			8.8			2302
9	90°	127x127x9.5	19.0	475			4.2			5.3			6.9			1020
10	90°	127x127x9.5	19.0	475			3.6			4.4			6.1			960
11	90°	127x127x9.5	19.0	475			3.2			3.9			5.8			840
12	90°	127x127x9.5	19.0	475			4.7			6.3			7.2			1140
13	90°	127x127x9.5	19.0	475			5.7			8.1			8.0			1200
14	90°	127x127x9.5	19.0	475			5.4			7.5			7.9			1207
15	90°	127x127x9.5	19.0	475			7.7			10.8			11.0			1494
16	90°	127x127x9.5	19.0	475			9.3			13.2			13.2			1578
17	90°	127x127x9.5	19.0	475			10.8			15.3			15.3			1788
Spec. No.	Angle between RHS and Plate	RHS Designation	t_p [mm]	l_w [mm]			Average of t_w [mm]			Average of w_b [mm]			Average of w_p [mm]			P_n [kN]
				at a&b	at c	at d	at a&b	at c	at d	at a&b	at c	at d	at a&b	at c	at d	
18	60°	127x127x9.5	19.0	137	119	119	6.1	4.2	8.3	8.0	8.4	10.8	9.4	8.6	8.8	1131
19	60°	127x127x9.5	19.0	137	119	119	3.8	2.7	5.2	5.6	5.4	6.1	5.3	5.6	6.0	982
20	60°	127x127x9.5	19.0	137	119	119	4.9	3.8	8.1	8.3	8.6	11.2	6.0	6.8	8.5	1270
21	60°	127x127x9.5	19.0	137	119	119	9.2	6.8	12.4	12.5	13.2	14.5	13.5	13.9	14.2	1534

*Locations a, b, c and d are indicated in Fig. 3.

Table 3. Measured geometric properties and connection failure loads for CHS-to-plate specimens

Spec. No.	Angle between RHS and Plate	CHS Designation	t_p [mm]	l_w [mm]	Average of t_w [mm]	Average of w_b [mm]	Average of w_p [mm]	P_n [kN]
22	90˚	168x7.1	25.0	527	3.90	5.91	5.22	1261
23	90˚	168x7.1	25.0	527	5.36	8.10	7.19	1279
24	90˚	127x13	25.0	400	6.09	8.60	8.75	1459
25	90˚	127x13	25.0	400	7.12	9.77	10.43	1597
26	90˚	102x8.0	25.0	318	4.07	5.67	5.91	841
27	90˚	102x8.0	25.0	318	4.04	5.91	5.58	864
28	60˚	168x7.1	25.0	569	3.67	5.45	5.33	1450
29	60˚	168x7.1	25.0	569	3.96	6.12	5.53	1331
30	60˚	127x13	25.0	432	5.06	7.19	7.43	1109
31	60˚	127x13	25.0	432	6.59	9.41	9.68	1479
32	60˚	102x8.0	25.0	342	3.77	5.73	5.46	776
33	60˚	102x8.0	25.0	342	3.49	5.19	5.03	803

Table 4. Measured material properties

Specimen No.	HSS		Plate		Weld Metal	
	F_y [MPa]	F_u [MPa]	F_{yp} [MPa]	F_{up} [MPa]	F_{yw} [MPa]	X_u [MPa]
1 through 4	412	478	383	563	563	619
5 through 8	380	489	383	563	563	619
9, 10, 11, 17 & 19	426	500	351	558	634	687
12, 13, 14, 15, 16, 18, 20 & 21	426	500	351	558	641	739
22, 23, 28, 29	421	501	409	566	501	571
24, 25, 30, 31	431	488	409	566	501	571
26, 27, 32, 33	385	450	409	566	501	571

Figure1

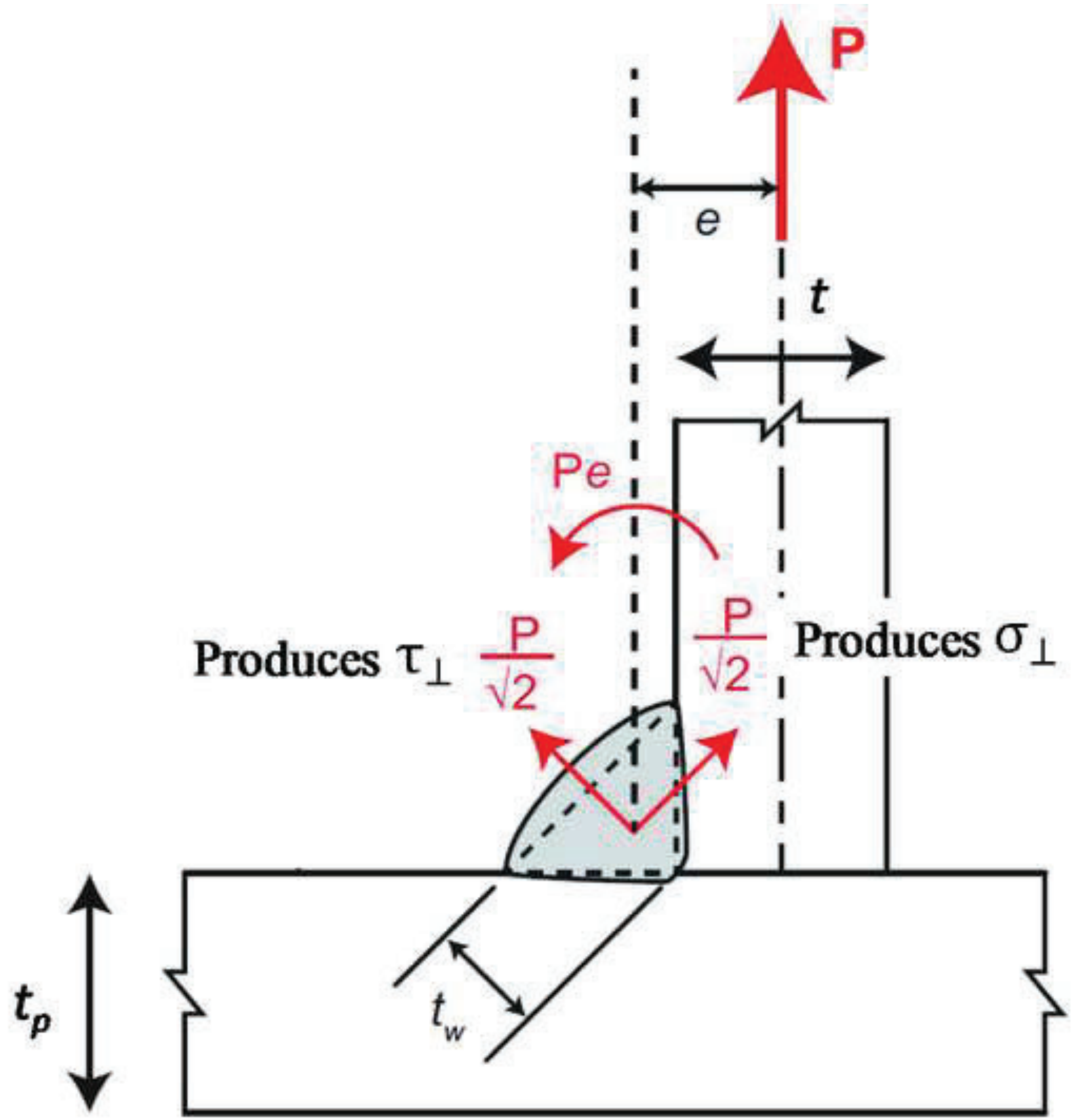
P
e
t
Pe
Produces $\tau_\perp$
$\frac{P}{\sqrt{2}}$
$\frac{P}{\sqrt{2}}$
Produces $\sigma_\perp$
t_p
t_w

Figure2

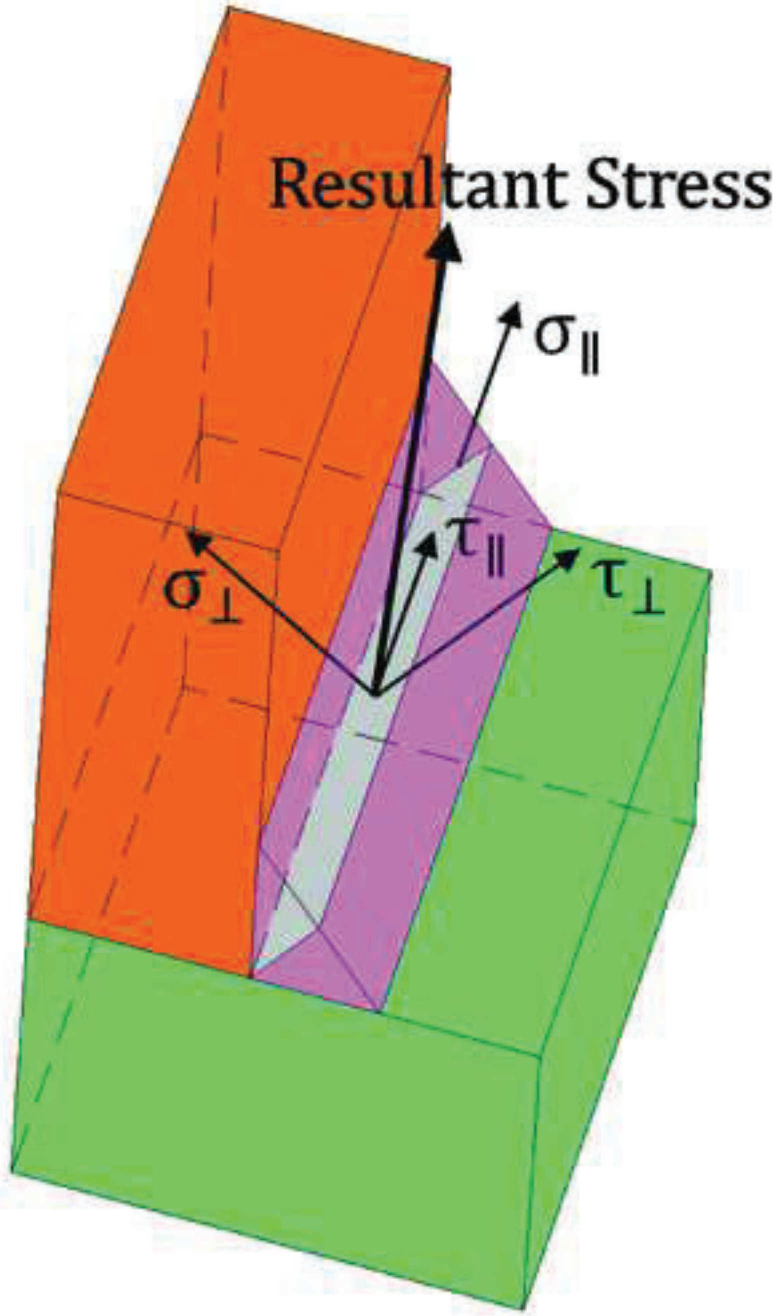
Resultant Stress
$\sigma_{\parallel}$
$\tau_{\parallel}$
$\tau_{\perp}$
$\sigma_{\perp}$

Figure3

Click here to download Figure Fig. 3-01.tif

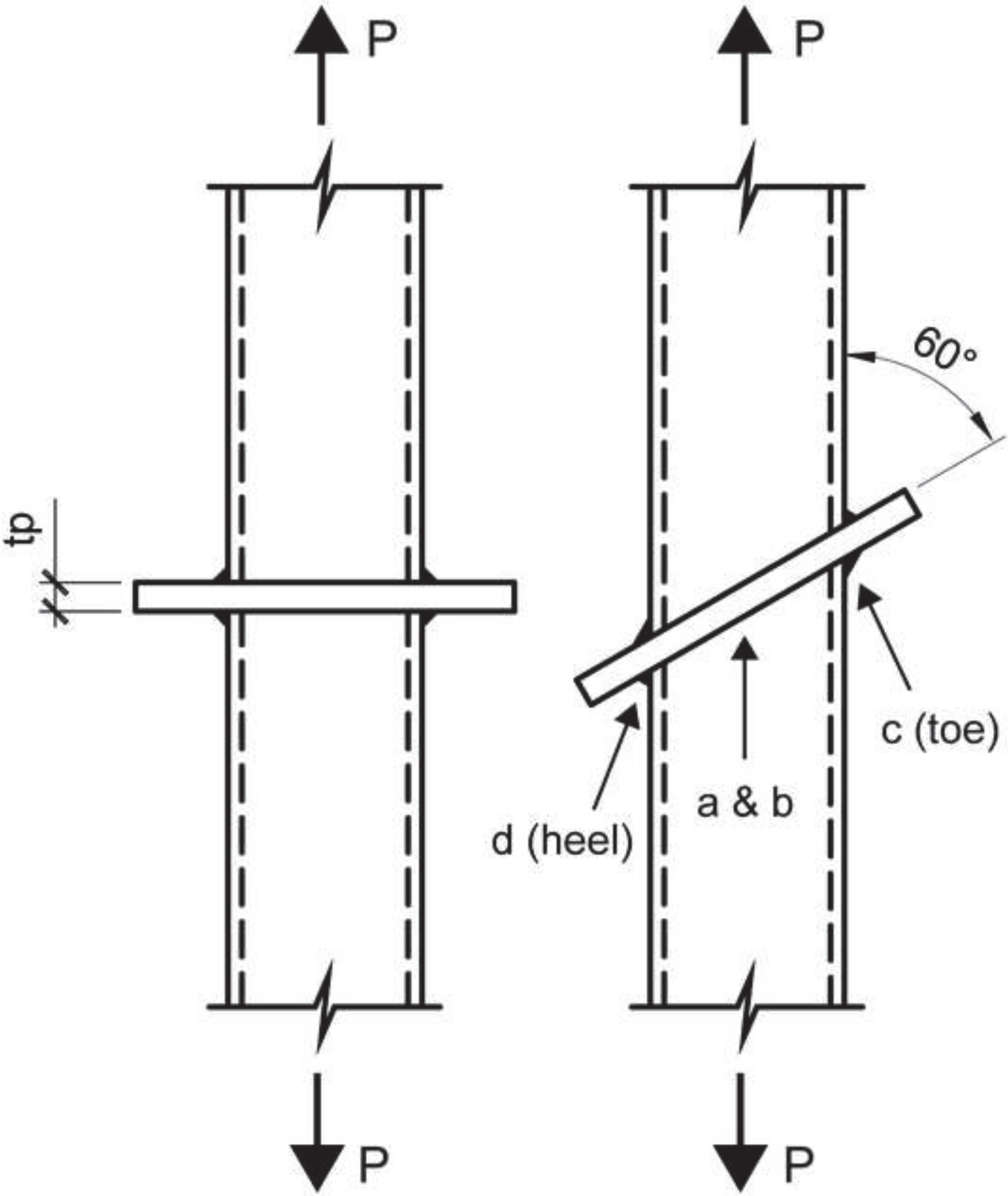

Figure4

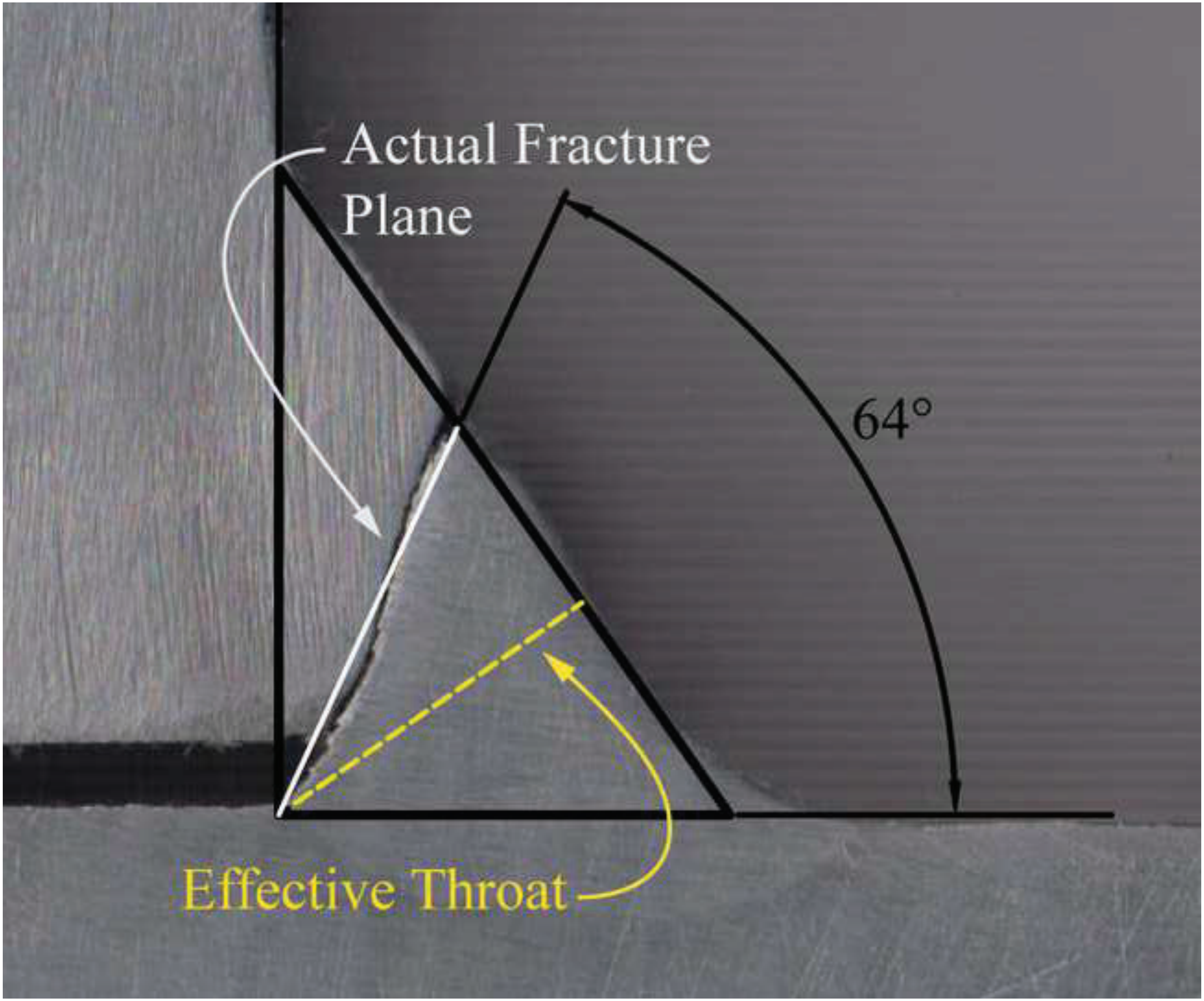

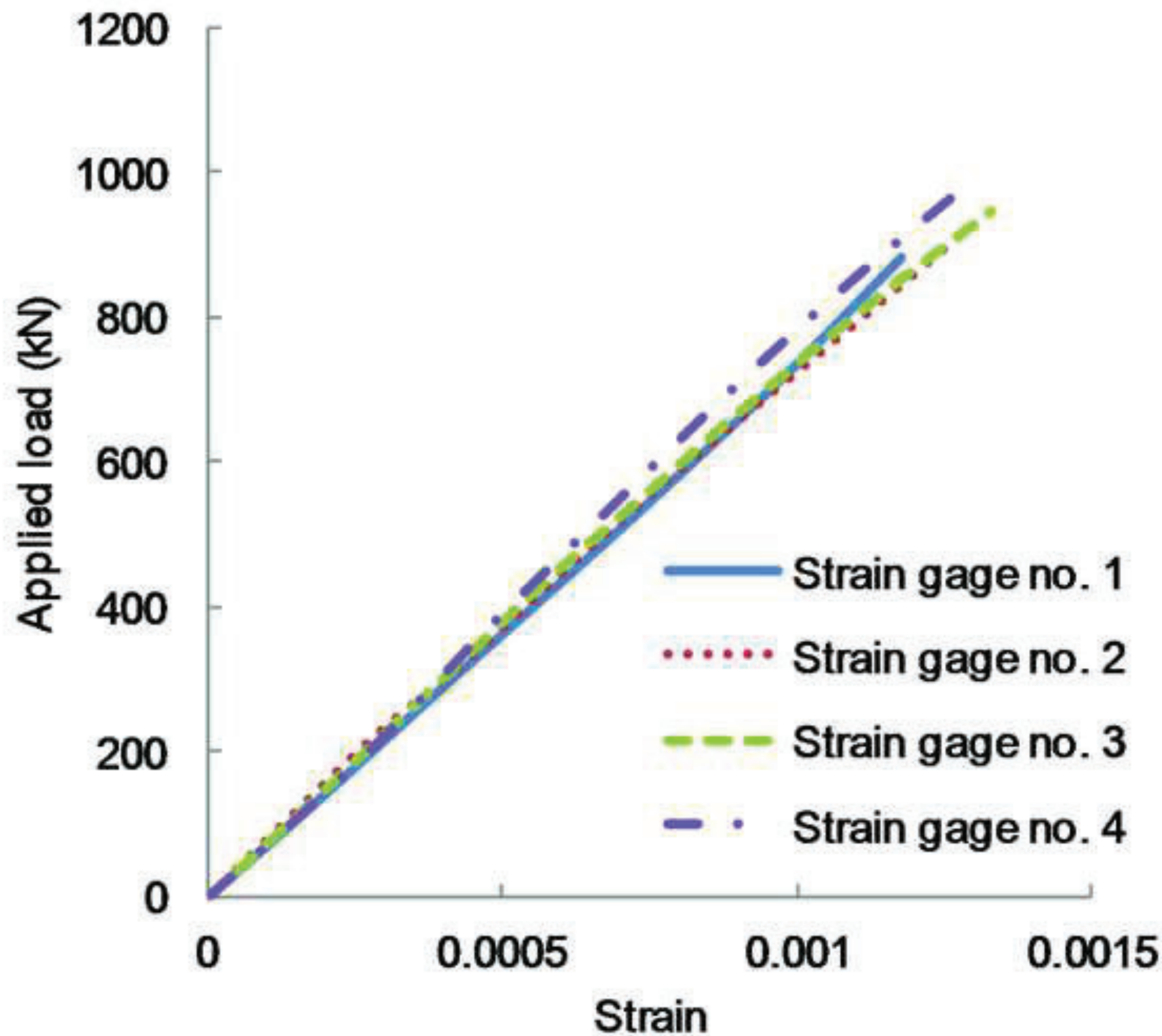
Applied load (kN)
1200
1000
800
600
400
200
0
0
0.0005
0.001
0.0015
Strain
Strain gage no. 1
Strain gage no. 2
Strain gage no. 3
Strain gage no. 4

Figure6

Click here to download Figure Fig. 6-01.tif

Figure7a

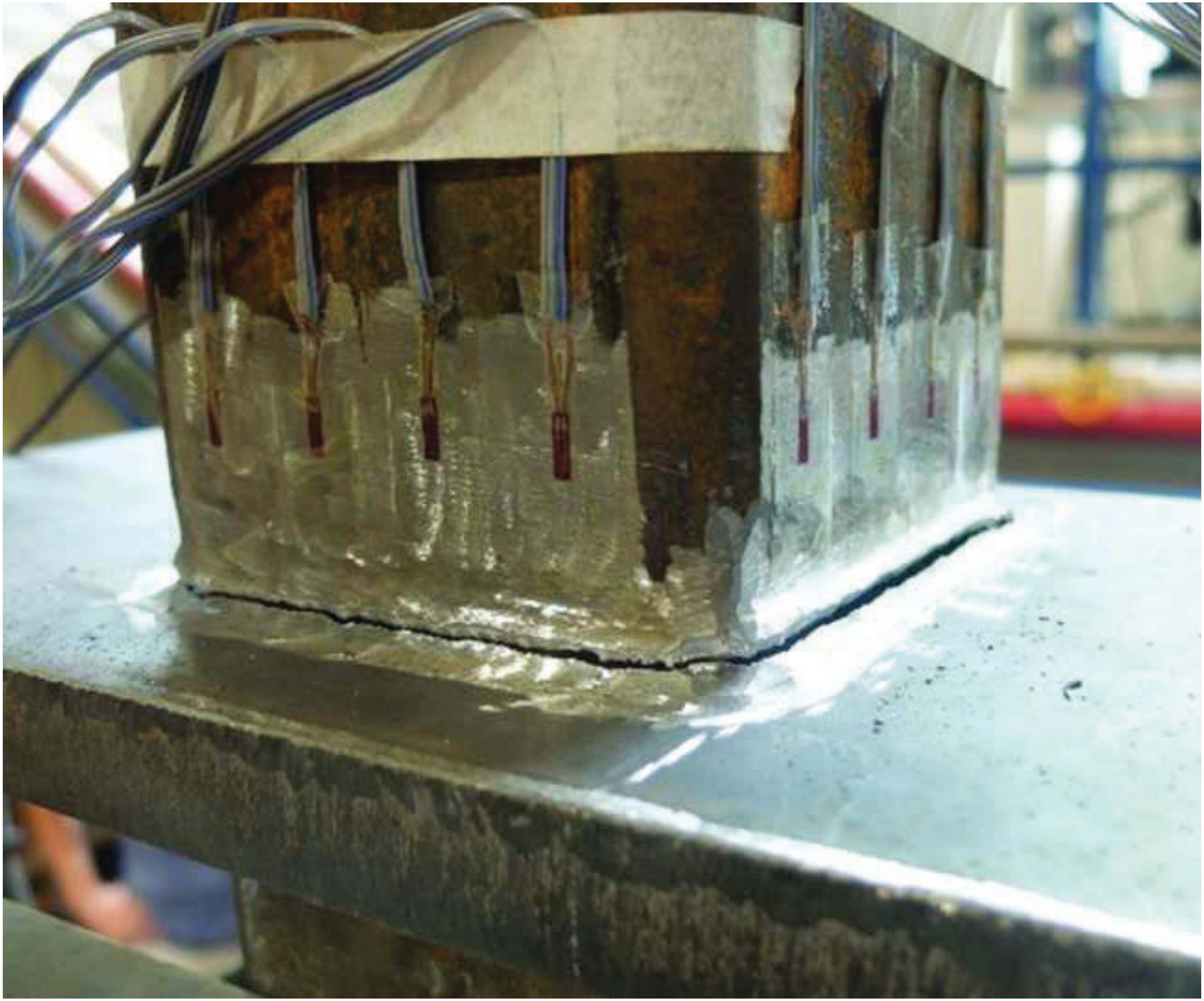

Figure7b

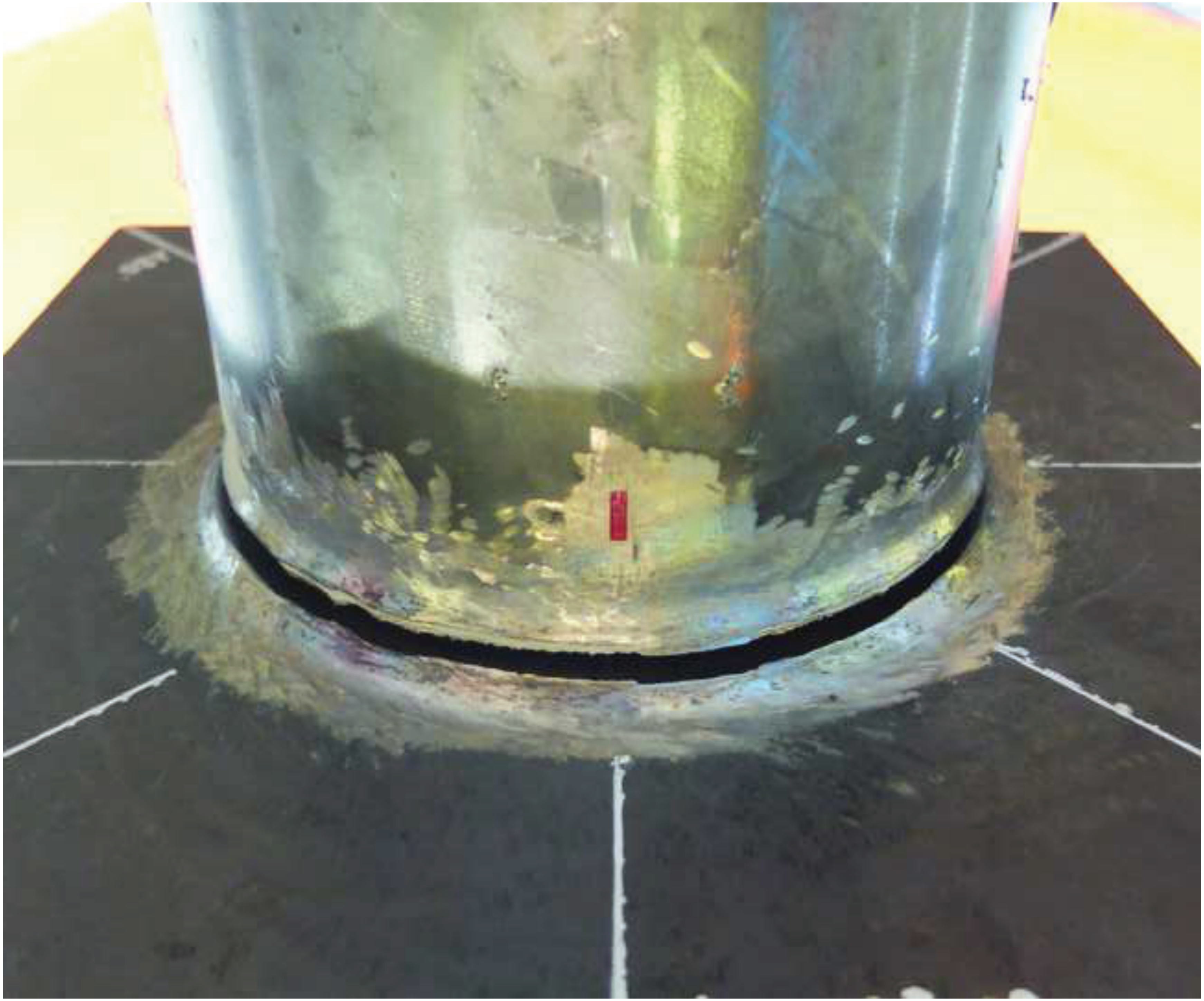

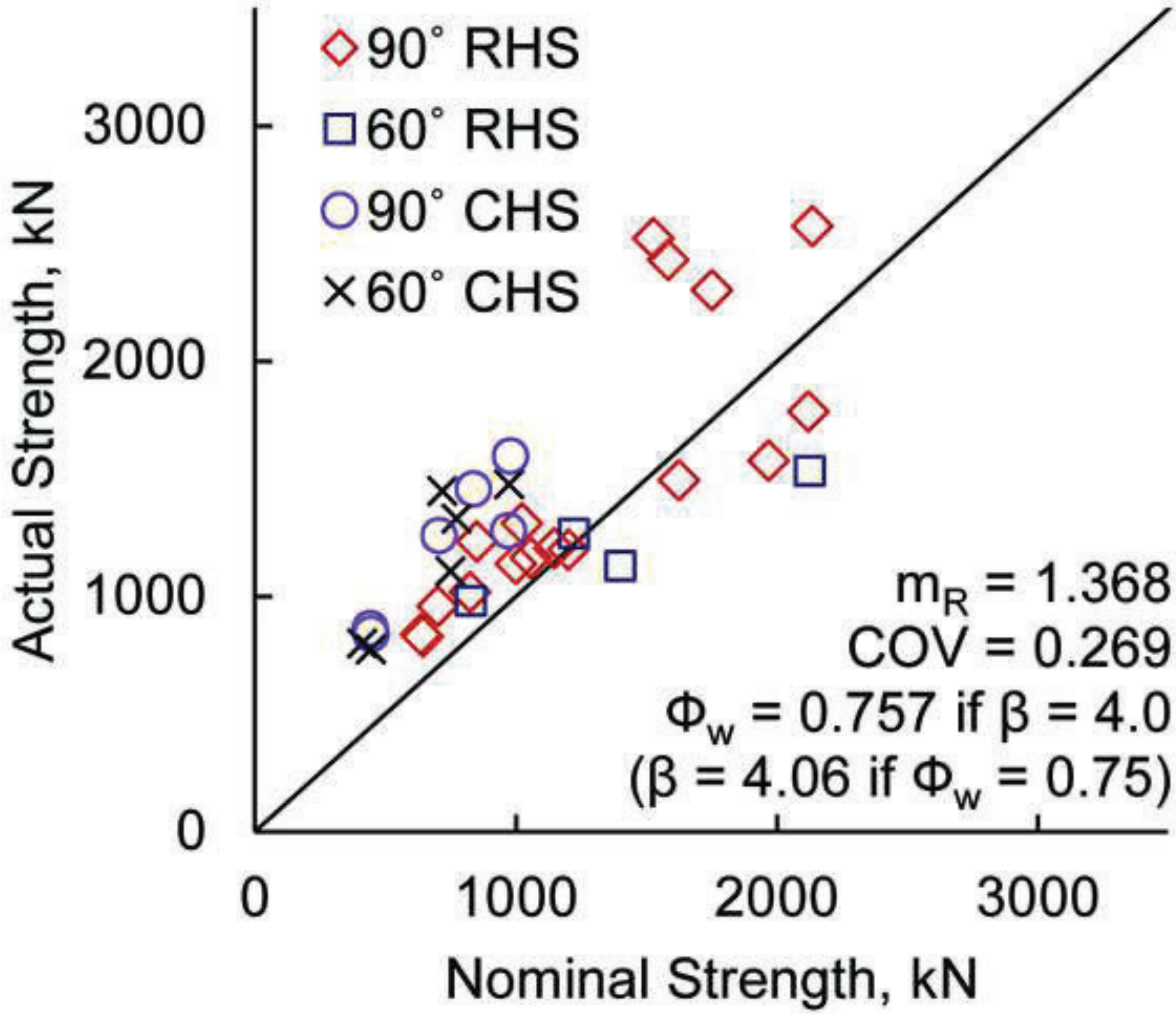
90° RHS
60° RHS
90° CHS
60° CHS
3000
2000
1000
0
Actual Strength, kN
0
1000
2000
3000
Nominal Strength, kN
m_R = 1.368
COV = 0.269
Φ_w = 0.757 if β = 4.0
(β = 4.06 if Φ_w = 0.75)

Figure9

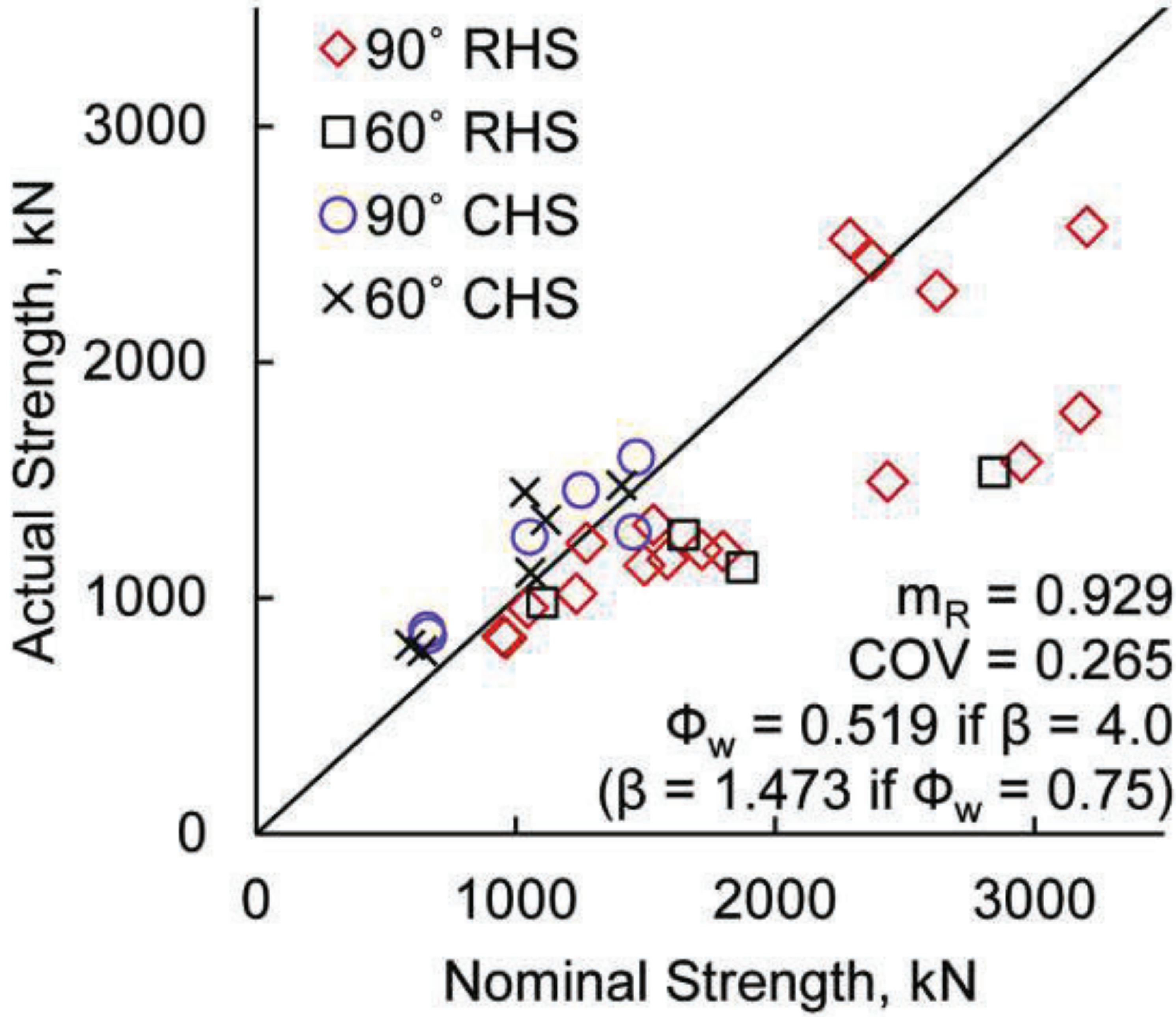
90° RHS
60° RHS
90° CHS
60° CHS
3000
2000
1000
0
Actual Strength, kN
0
1000
2000
3000
Nominal Strength, kN
m_R = 0.929
COV = 0.265
Φ_w = 0.519 if β = 4.0
(β = 1.473 if Φ_w = 0.75)

Figure10

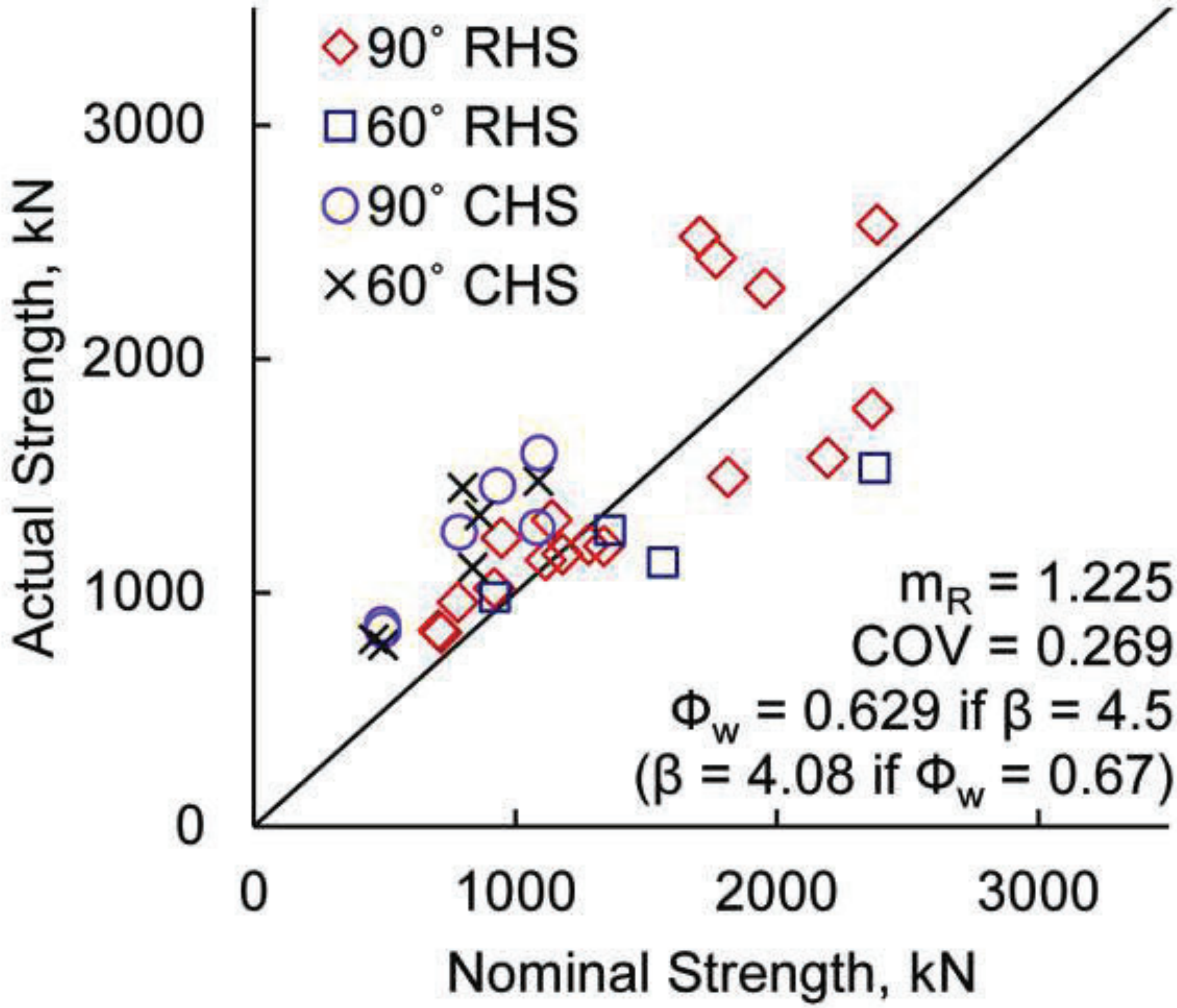
90° RHS
60° RHS
90° CHS
60° CHS
3000
2000
1000
0
Actual Strength, kN
0
1000
2000
3000
Nominal Strength, kN
m_R = 1.225
COV = 0.269
Φ_w = 0.629 if β = 4.5
(β = 4.08 if Φ_w = 0.67)

Figure11

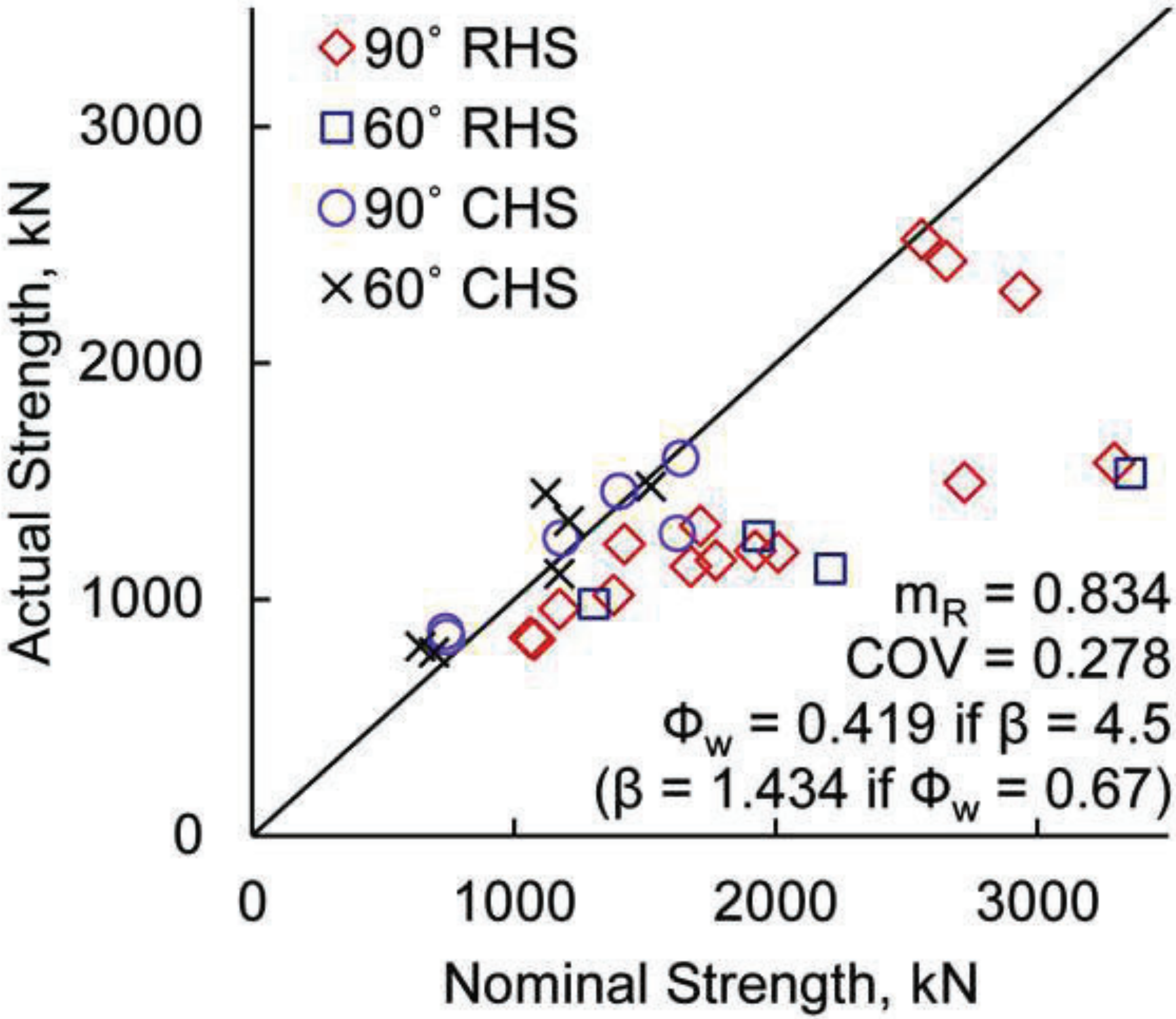
90° RHS
60° RHS
90° CHS
60° CHS
3000
2000
1000
0
Actual Strength, kN
0
1000
2000
3000
Nominal Strength, kN
m_R = 0.834
COV = 0.278
Φ_w = 0.419 if β = 4.5
(β = 1.434 if Φ_w = 0.67)

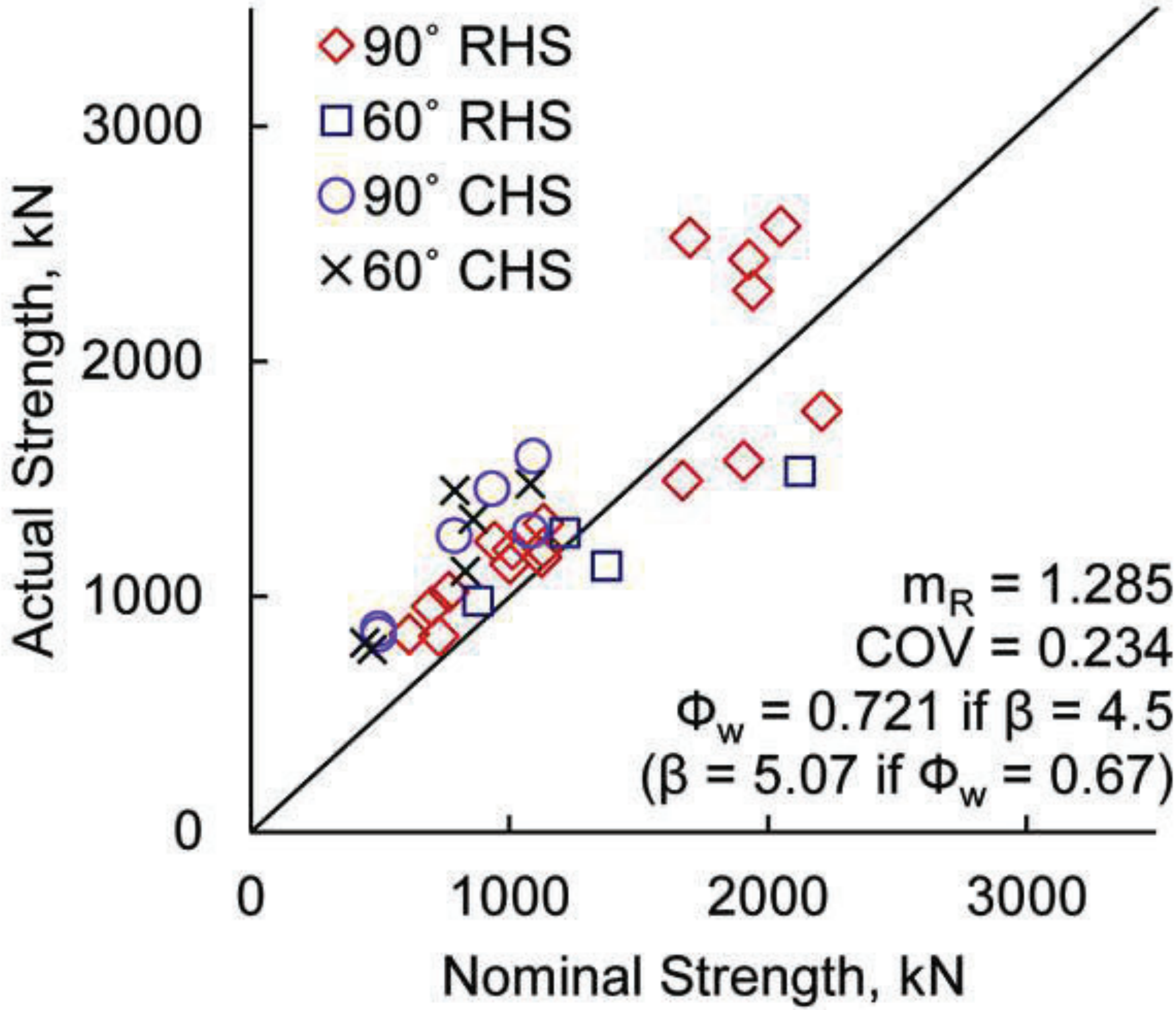
90° RHS
60° RHS
90° CHS
60° CHS
3000
2000
1000
0
Actual Strength, kN
0
1000
2000
3000
Nominal Strength, kN
m_R = 1.285
COV = 0.234
Φ_w = 0.721 if β = 4.5
(β = 5.07 if Φ_w = 0.67)

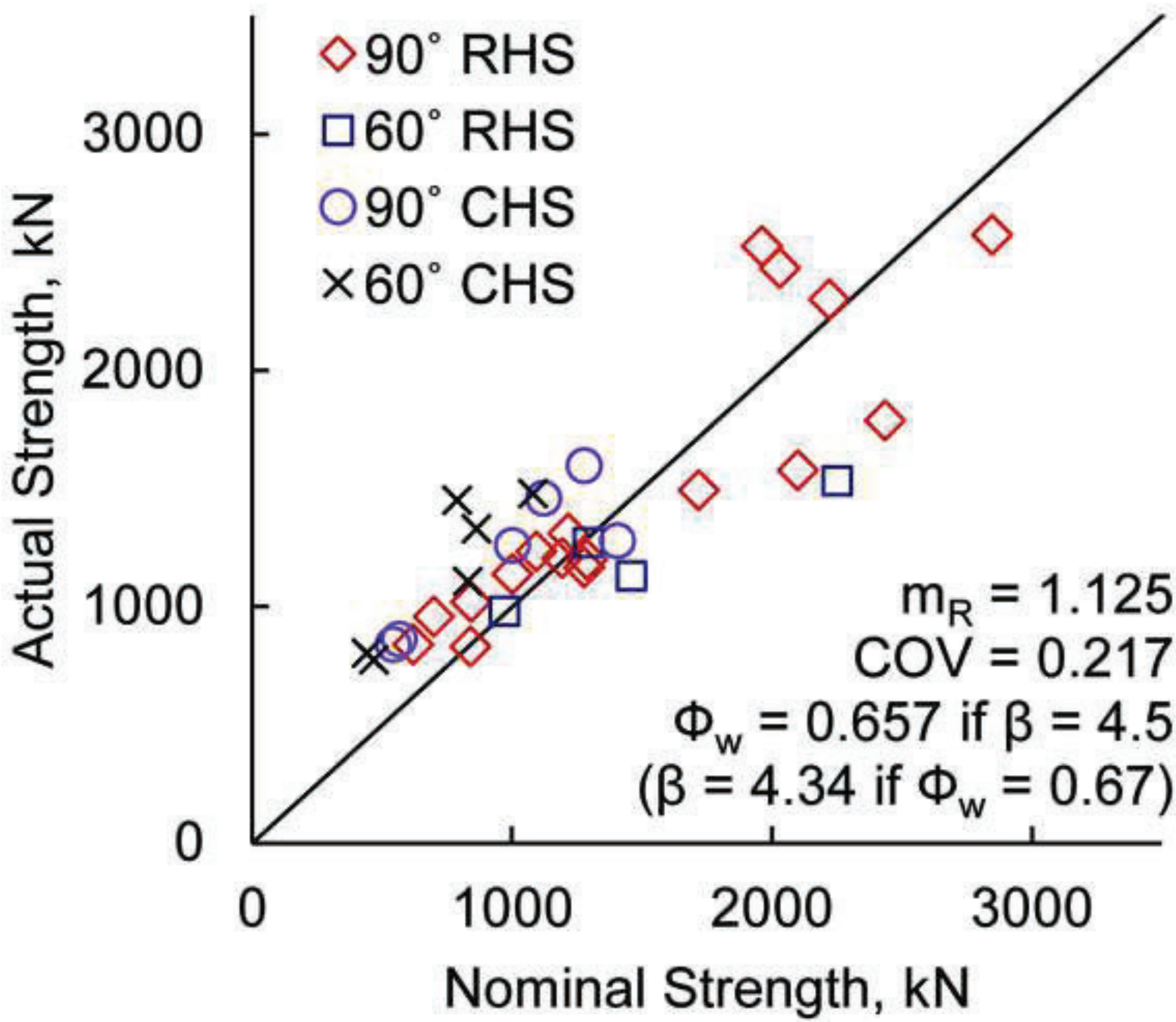
90° RHS
60° RHS
90° CHS
60° CHS
3000
2000
1000
0
Actual Strength, kN
0
1000
2000
3000
Nominal Strength, kN
m_R = 1.125
COV = 0.217
Φ_w = 0.657 if β = 4.5
(β = 4.34 if Φ_w = 0.67)

Figure14

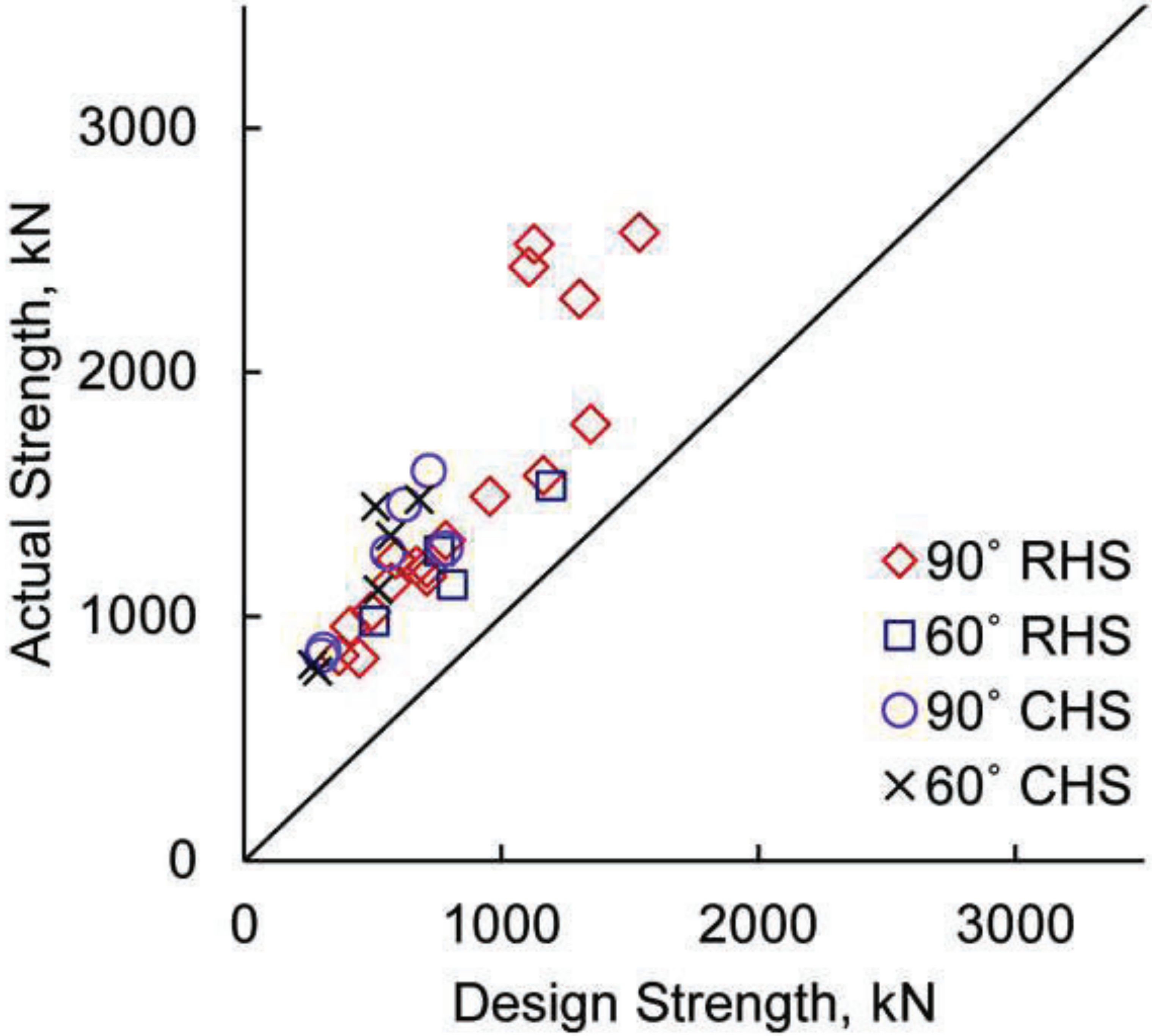

Actual Strength, kN
3000
2000
1000
0
0
1000
2000
3000
Design Strength, kN
90° RHS
60° RHS
90° CHS
60° CHS

Figure15

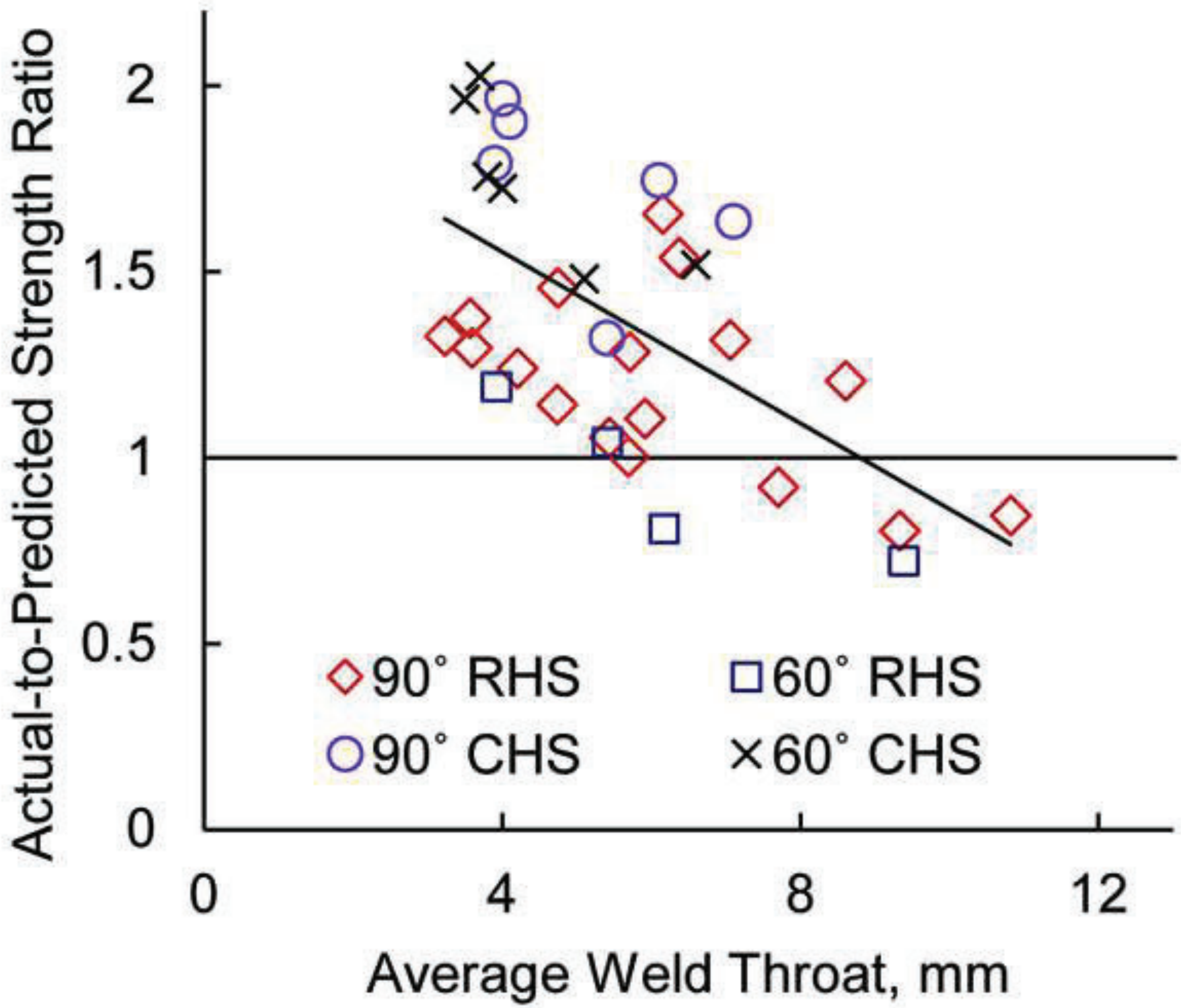
Actual-to-Predicted Strength Ratio
2
1.5
1
0.5
0
0
4
8
12
Average Weld Throat, mm
90° RHS
60° RHS
90° CHS
60° CHS

Figure16

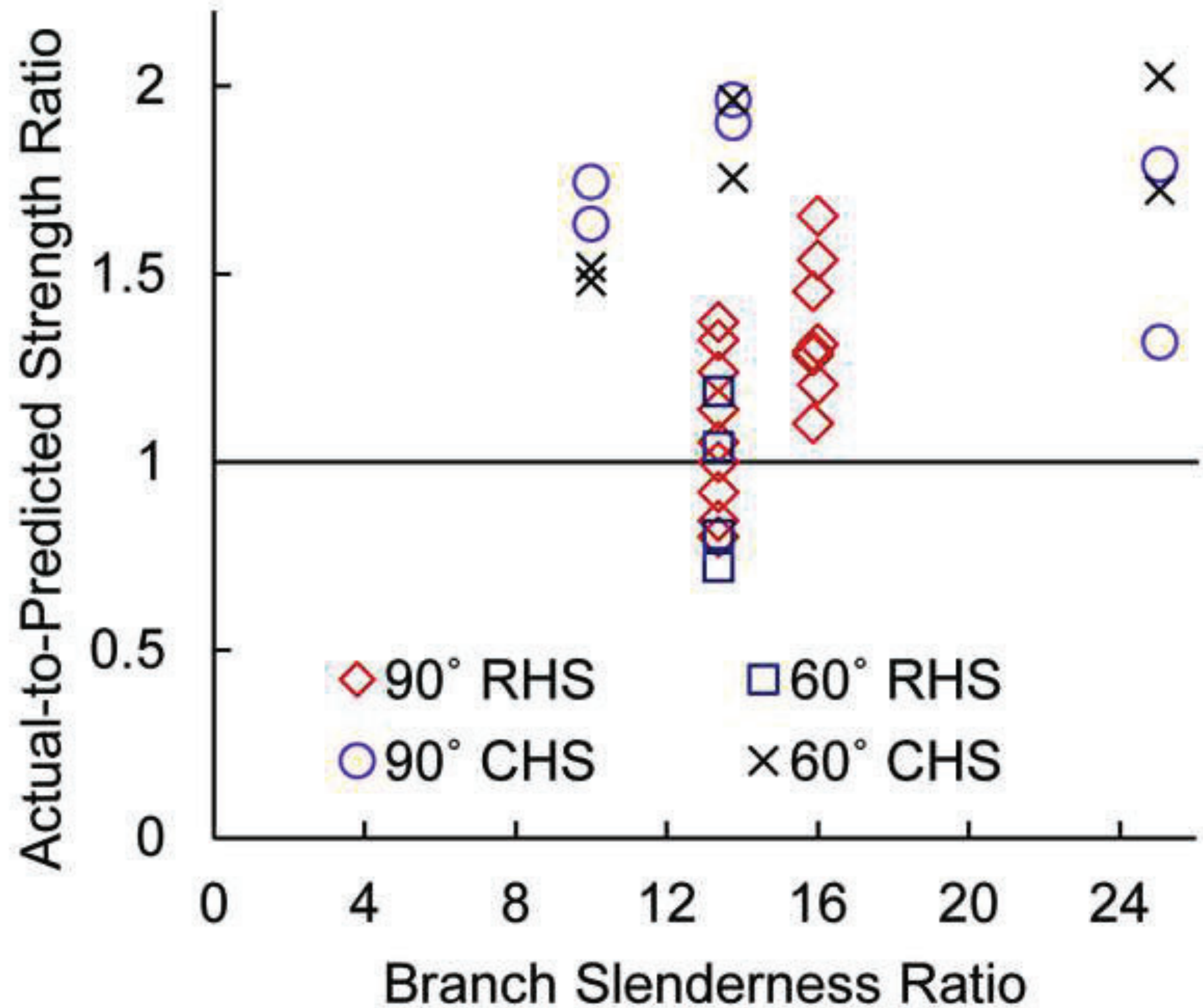

Actual-to-Predicted Strength Ratio
2
1.5
1
0.5
0
0
4
8
12
16
20
24
Branch Slenderness Ratio
90° RHS
60° RHS
90° CHS
60° CHS